Allelic Variation, Aneuploidy, and Nongenetic Mechanisms Suppress a Monogenic Trait in Yeast

Amy Sirr, Gareth A. Cromie, Eric W. Jeffery, Teresa L. Gilbert,[1] Catherine L. Ludlow, Adrian C. Scott, and Aimée M. Dudley[2]
Pacific Northwest Diabetes Research Institute, Seattle, Washington 98122

ABSTRACT Clinically relevant features of monogenic diseases, including severity of symptoms and age of onset, can vary widely in response to environmental differences as well as to the presence of genetic modifiers affecting the trait's penetrance and expressivity. While a better understanding of modifier loci could lead to treatments for Mendelian diseases, the rarity of individuals harboring both a disease-causing allele and a modifying genotype hinders their study in human populations. We examined the genetic architecture of monogenic trait modifiers using a well-characterized yeast model of the human Mendelian disease classic galactosemia. Yeast strains with loss-of-function mutations in the yeast ortholog (*GAL7*) of the human disease gene (*GALT*) fail to grow in the presence of even small amounts of galactose due to accumulation of the same toxic intermediates that poison human cells. To isolate and individually genotype large numbers of the very rare (~0.1%) galactose-tolerant recombinant progeny from a cross between two *gal7*Δ parents, we developed a new method, called "FACS-QTL." FACS-QTL improves upon the currently used approaches of bulk segregant analysis and extreme QTL mapping by requiring less genome engineering and strain manipulation as well as maintaining individual genotype information. Our results identified multiple distinct solutions by which the monogenic trait could be suppressed, including genetic and nongenetic mechanisms as well as frequent aneuploidy. Taken together, our results imply that the modifiers of monogenic traits are likely to be genetically complex and heterogeneous.

MEDICAL genetics is based on the assumption that the sequence of a gene (or complete genome) can be used to predict an individual's phenotype(s), including traits related to the prevention, diagnosis, and treatment of human disease. The most success in this regard has come from the analysis of monogenic (Mendelian) traits, *i.e.*, those linked to polymorphisms in a single gene. The Online Mendelian Inheritance in Man database currently contains ~3000 human genes "with a phenotype-causing mutation" (http://omim.org/), including many diseases caused by complete or partial loss of gene function. Inborn errors of metabolism (IEMs), such as cystic fibrosis and galactosemia, are often monogenic diseases that are individually rare but common as a class (in the United States at least 1 in 5000 live births is affected by an IEM) (Gupta 2007). In contrast, many common diseases such as asthma, diabetes, heart disease, and cancer show heritability patterns that suggest the involvement of large numbers of genes and environmental factors (Akhabir and Sandford 2011; Hindorff *et al.* 2011; Marian and Belmont 2011; Polychronakos and Li 2011). While the fundamental concepts of mapping these so-called complex traits, or quantitative trait loci (QTL), were introduced decades ago (Lander and Botstein 1989), attempts to identify and understand the underlying genes have met with limited success. QTL analysis in humans and model organisms typically detects only a fraction of the predicted number of loci. A commonly cited example is that of human height in which all genetic loci identified to date explain only 10% of the phenotypic variation (Lango Allen *et al.* 2010).

When examined closely, the division between monogenic and complex traits quickly breaks down. Clinically relevant features of monogenic diseases, including severity of symptoms and age of onset, vary widely in response to environmental differences and the presence of genetic modifiers that affect the penetrance and expressivity of the trait (Dipple and McCabe 2000b; Nadeau 2001; Weatherall 2001; Genin *et al.* 2008).

doi: 10.1534/genetics.114.170563
Manuscript received September 5, 2014; accepted for publication November 11, 2014; published Early Online November 13, 2014.
Available freely online through the author-supported open access option.
Supporting information is available online at http://www.genetics.org/lookup/suppl/doi:10.1534/genetics.114.170563/-/DC1.
[1]Deceased.
[2]Corresponding author: Pacific Northwest Diabetes Research Institute, 720 Broadway, Seattle, WA 98122. E-mail: aimee.dudley@gmail.com.

Thus, monogenic diseases can be viewed as a special class of complex trait in which allelic variation in one gene has an overwhelmingly strong effect over one or more independently inherited modifier gene(s) that exacerbate or ameliorate the primary disease gene's phenotype. Because some modifiers confer protective effects against the underlying disease allele or causative agent, understanding them may reveal means of reducing the adverse effects of deleterious polymorphisms (Nadeau 2003).

Like other complex traits, identifying modifiers of monogenic diseases has generally been "a frustration and disappointment to clinical geneticists, who hoped that knowledge of a patient's genotype would predict disease and optimize prevention" (Dipple and McCabe 2000a). Because Mendelian diseases are often rare in the human population and individuals with similar sets of modifiers are (presumably) even rarer (Knowles 2006; Weiler and Drumm 2013), some of these failings may be due to the lack of statistical power (sufficiently large numbers of individuals). Studies in model organisms have the potential to overcome this limitation, particularly through the use of large-scale crosses. *Saccharomyces cerevisiae* is ideally suited to this type of analysis due to its ease of propagation, genetic manipulability, high meiotic recombination rate, well-characterized genome, and abundance of genetic resources and large-scale data sets (Botstein and Fink 2011). The conservation of core cellular pathways, such as metabolism between yeast and humans, provides a powerful system for the study of human disease gene orthologs. Thus, the application of QTL mapping methods to large-scale crosses of yeast with specific gene deletions could identify loci capable of modifying medically relevant monogenic traits.

Large-scale trait-mapping methods that have been developed for *S. cerevisiae* generally differ from one another in two respects: (1) whether the entire population of recombinant progeny or an extreme tail of the phenotype distribution is recovered and (2) whether genotyping is performed on individuals or in pools. To reduce the high cost of genotyping, several studies (Segre *et al.* 2006; Dunham 2012) have leveraged a pooled genotyping strategy known as bulked segregant analysis (BSA) (Michelmore *et al.* 1991) to detect QTL enriched in individuals displaying the trait of interest. Extensions of this method, such as extreme QTL mapping (X-QTL) (Ehrenreich *et al.* 2010), are designed to examine the genetics underlying rare phenotypes, which reside in the extreme tail of the phenotype distribution. These approaches perform pooled genotyping following a strong phenotypic selection imposed on an extremely large initial pool of recombinant progeny, for example, a drug concentration that kills 99% of progeny. In some cases additional rounds of selection are used on intercrossed populations to narrow the linked regions (Parts *et al.* 2011).

Despite their ease of use, these methods have a few limitations. First, genotyping populations *en masse* (rather than as individuals) is confounded by genetic heterogeneity, *i.e.*, multiple, distinct genetic solutions with a similar phenotype (Wilkening *et al.* 2013). Second, commonly used methods employ a set of auxotrophic markers and multiple selective plating steps to isolate large numbers of recombinant haploid progeny away from the pool of vegetative (heterozygous diploid) cells. Finally, these auxotrophies themselves have the potential to influence the trait of interest. With these challenges in mind, we previously developed the Barcode Enabled Sequencing of Tetrads (BEST) method (Ludlow *et al.* 2013; Scott *et al.* 2014). BEST avoids the use of auxotrophies, recovers the entire population of recombinant progeny from a cross, and through the use of a molecular barcode retains tetrad (sister spore) relationship information.

In this study, we develop a genetic mapping technique called fluorescence-activated cell sorting (FACS)-QTL (Figure 1), which permits the isolation of extremely large numbers of recombinant progeny that can then be subjected to strong phenotypic selections. Like BEST, FACS-QTL uses a sporulation-specific GFP reporter gene to isolate tetrads by FACS, but because FACS-QTL does not leverage sister-spore information, the high-complexity barcodes used in BEST are unnecessary and the reporter gene can be stably integrated into the parental genomes. Once tetrads are isolated, they are disrupted during plating directly onto the selective medium, and individual colonies passing the stringent selection are individually genotyped. To demonstrate the utility of FACS-QTL, we used it to study genetic modifiers in a yeast model of a human disease, galactosemia.

In humans, classic galactosemia is a monogenic, autosomal recessive condition caused by loss-of-function mutations in the gene encoding galactose-1-phosphate uridylyltransferase (*GALT*), an enzyme in the Leloir pathway (Mayatepek *et al.* 2010; McCorvie and Timson 2011). The impaired activity of GALT in galactosemic individuals results in a broad range of side effects believed to result from the accumulation of toxic intermediates, such as galactitol and galactose-1-phosphate (Leslie 2003; Tang *et al.* 2012). Classic galactosemia can be modeled in *S. cerevisiae* by deleting the *GALT* ortholog *GAL7* (Figure 2) (Douglas and Hawthorne 1964). In these mutants, the presence of even low levels of galactose inhibits cell growth owing to toxic accumulation of the same metabolites (De Jongh *et al.* 2008; Mumma *et al.* 2008). By applying FACS-QTL to a cross between two *gal7*Δ strains, we were able to identify several means by which the effect of the major locus could be suppressed. These solutions included major-effect QTL, nongenetic effects, a surprisingly high level of aneuploidy, and an allele–aneuploidy interaction. Our results emphasize the advantages of maintaining individual genotype information in the presence of trait complexity and heterogeneity.

Materials and Methods

Strains and growth conditions

Unless noted, standard media and methods were used to grow and manipulate yeast (Rose *et al.* 1990). Strains used

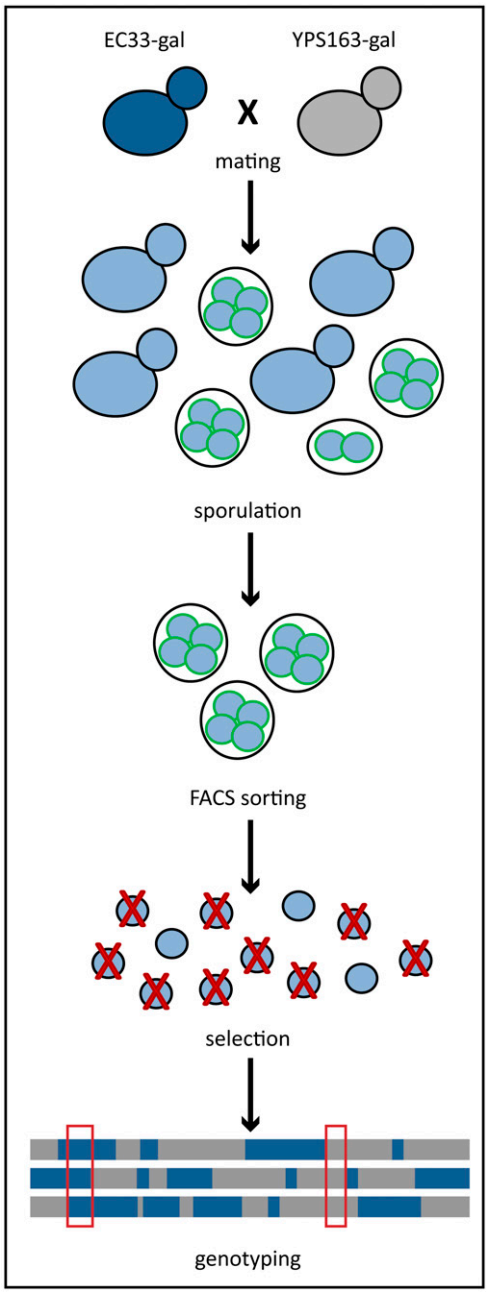

Figure 1 FACS-QTL mapping method. Two natural variant strains are selected based on their genetic dissimilarity and the trait of interest. Prototrophic parent strains are tagged with a sporulation-specific GFP marker and crossed, enabling large numbers of tetrads to be isolated from unsporulated diploids and dyads by flow cytometry. Tetrads are then disrupted and individual haploid progeny are grown under selective conditions. Spores capable of overcoming selection are individually sequenced using a multiplexed RAD-seq method. Regions of biased allele inheritance among the selected progeny can then be identified, as indicated by red boxes, by QTL mapping.

in this study (Table 1) were grown at 30° in YPD (2% glucose) unless otherwise noted. Drug resistance markers were selected on YPD supplemented with standard concentrations of G418, nourseothricin, or hygromycin (Wach *et al.* 1994; Goldstein and McCusker 1999). For QTL mapping, spores were plated on YPD, YPRaf (YEP with 2% raffinose and 1 μg/ml antimycin A), and YEP with 0.05% galactose, 2% raffinose, and 1 μg/ml antimycin A. Progenitor strains of our initial cross, EC-33 (gift of Eviatar Nevo) and YPS163 (gift of Justin Fay), were prescreened for robust growth on YPD, YPGal (2% galactose), YPG (3% glycerol), and synthetic dextrose minimal media (SD) (Guthrie and Fink 1991).

Growth rates were determined using a minimum of eight replicates grown at 30° in a microplate absorbance reader (Tecan Sunrise) set at 600 nm in accuracy mode with high-intensity shaking. Measurements were taken every 15 min for a minimum of 24 hr. Strains were inoculated in the media at a density of 10^5 cells/ml using cultures grown overnight in YPRaf at 30° and sonicated briefly. Doubling times were calculated using linear regression carried out on the log-transformed absorbance measurements with a sliding window of four intervals (1 hr) to determine the maximum growth rate of each replicate.

Yeast strain construction

Strain construction was performed as follows. Briefly, the *HO* locus was disrupted using the *HphMX6* cassette (Goldstein and McCusker 1999) in homozygous, homothallic diploid isolates derived from nonlaboratory strains. After sporulation and dissection, heterothallic haploids were identified by hygromycin resistance, and *HO* deletion was confirmed by PCR. Haploids were tagged at a sporulation-specific locus using an *SPS2*:*EGFP:KanMX4* cassette for *MAT***a** isolates and an *SPS2*:*EGFP:NatMX4* cassette for *MATα* isolates (Gerke *et al.* 2006). The *SPS2* cassettes were PCR-amplified from strains BC235 and BC237 (gifts of Barak Cohen) using primers AO45 (5′-GATCTCACTAAGAATTGAAGC-3′) and AO46 (5′-TTAACCCTAAGGAAGAACCG-3′), which bear homology to the upstream and downstream regions of the native *SPS2* locus.

Using this strategy, *MAT***a** strain YO528 was derived from initial isolate EC-33. In a similar manner, the *MATα* heterothallic haploid strain YPS163 (*ho*Δ::*dsdAMX4*) was tagged at *SPS2* with the *SPS2:EGFP:NatMX4* cassette to create strain YO516. To conserve markers for this study, the *KanMX4* cassette in strain YO528 was replaced with *NatMX4* using *Eco*RI-linearized p4339 (Tong *et al.* 2001) (gift of Charles Boone), generating strain YO794. Strains YO795 and YO796 were derived from YO794 and YO516 by deleting *GAL7* with a *gal7Δ0*::*KanMX4* cassette PCR-amplified from the *MAT***a** deletion library (Wach *et al.* 1994).

To add an extra copy of *GAL80* to parental strains, an integrating plasmid containing *GAL80* and its native promoter, pEL17 (gift of Fred Winston), was linearized at a unique site in the *URA3* promoter region with *Nde*I (Larschan and Winston 2005) and transformed into the strain YO1012 to create strains YO1457, YO1458, and YO1459 (from Evolution Canyon background) and into strain YO964 to create strains YO1454, YO1455, and YO1456 (Oak background).

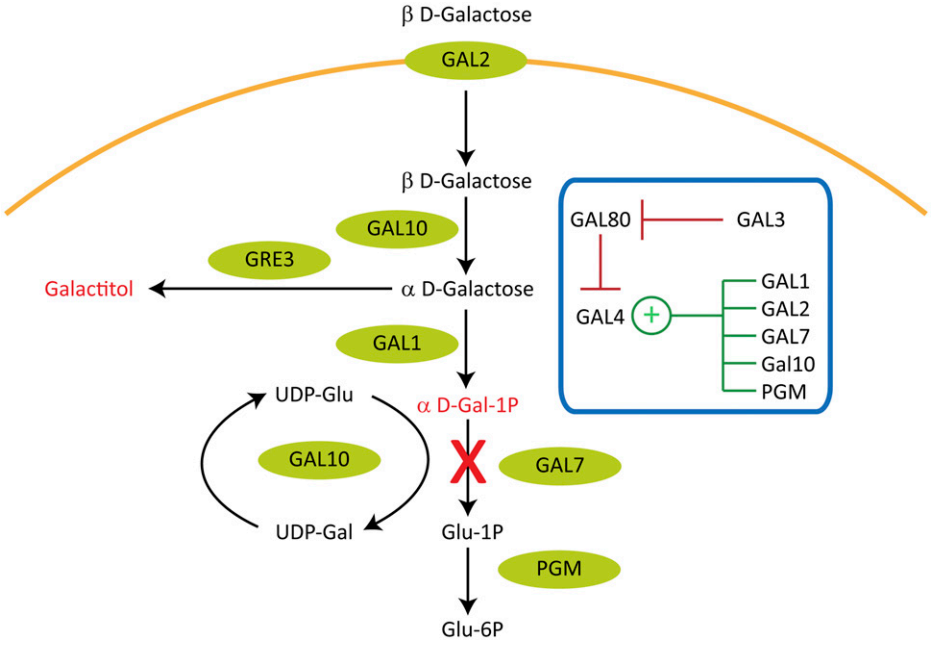

Figure 2 Galactose utilization pathway in the *S. cerevisiae* model of galactosemia. Galactose enters the cell through the galactose permease Gal2p. Yeast pathway enzymes Gal1p, Gal7p, Gal10p, Pgm1p, and Pgm2p metabolize galactose into glucose-6-P in a manner almost identical to the orthologous Leloir pathway in humans. Deletion of *gal7* leads to the buildup of the toxic metabolites galactitol and D-galactose-1P (indicated in red). In *S. cerevisiae*, the galactose pathway is induced by the transcription factor Gal4p, which is repressed by Gal80p when yeast's preferred carbon source, glucose, is present. In the absence of glucose and the presence of galactose, Gal3p interacts with Gal80p to relieve the repression of Gal4p, inducing transcription of all galactose pathway genes.

Homozygous diploids were created from the heterothallic haploid segregants as follows. The *URA3* locus was deleted and strains were transformed with the *URA3*-marked plasmid pGAL-*HO* (Herskowitz and Jensen 1991) (gift of Timothy Galitski). Transcription of the HO endonuclease was induced with a concentration of galactose (0.05% galactose, 2% raffinose) that the segregants could tolerate without substantial toxicity for 4 hr. Cells were then plated onto YPD, and diploid isolates of the transformation were grown overnight in YPD and plated onto 5-FOA medium to facilitate plasmid loss.

Crosses

Strains YO795 and YO796 were crossed on YPD, and a single diploid colony, YO797, was patched onto pre-sporulation medium. A high percentage of dyads was observed in this cross, a characteristic previously noted in some natural variant wine strains (Gerke *et al.* 2006). To minimize dyad formation for this cross, ~6×10^8 cells/ml were sporulated in 4% potassium acetate for 2 days at room temperature. Sporulation conditions for each subsequent cross were optimized using similar conditions or sporulation on plates (Tong and Boone 2005; Xiao 2006). Sporulation efficiency was calculated as a percentage of tetrads formed among 200 cells counted in a 2-day-old sporulation culture. Approximately 3×10^6 tetrads were sorted for the initial cross on a FACSAria II (BD Bioscience), while 10^5–10^6 tetrads were sorted for subsequent backcrosses and intercrosses in a manner previously described (Ludlow *et al.* 2013; Scott *et al.* 2014).

Isolated tetrads were disrupted using a method modified from X-QTL analysis (Ehrenreich *et al.* 2010). Tetrads were pelleted and resuspended in 100 μl zymolyase (1 mg/ml in 0.7 M sorbitol) and incubated for 1 hr at 30° on a roller (Model TC-7, New Brunswick Scientific) followed by a 10-min incubation at 37°. Approximately 100 μl of glass beads and 450 μl of PBS were added to the cell suspension followed by 2 min of moderate vortexing. Spores were agitated on a roller for an additional hour at 30° followed by another 2 min of vortexing. Spores were checked under the microscope for tetrad disruption and to approximate cell numbers prior to spreading 10^2–10^5 cells on control and selection plates. Colonies were counted on day 2 and day 4. After 4 days on selective medium, segregants were picked and grown 2 days in YPD in a 96-well plate for sequencing and frozen stocks. Frequencies of galactose-tolerant individuals were calculated as the ratio of colonies counted on galactose medium to colonies counted on rich medium.

To characterize the unselected population, the parental diploid YO797 was sporulated, and a control population of 44 tetrads was hand-dissected on YPD using a micromanipulator. Each spore from this dissection was also individually restriction site-associated DNA (RAD)-sequenced.

Parental genome sequencing

The two progenitor strains YO516 and YO528 were whole-genome-sequenced (File S8) as follows. High-purity yeast DNA was prepared using a YeaStar Genomic DNA extraction kit (Zymo Research). DNA sequencing libraries were prepared using the Paired-End sequencing kit (Illumina) following the manufacturer's instructions. Sequence runs were performed on a Genome Analyzer IIx (Illumina) for 2- × 40-bp length reads multiplexing seven samples per flow cell lane. Reads were aligned to the S288c reference genome (R64-1-1) using BWA (v5.8) (Li and Durbin 2009), allowing six mismatches and using quality trimming (threshold of Phred = 20). SAMtools (v0.1.18) (Li *et al.* 2009) was then used to generate a pileup file for each parental strain, using the -C 50 and -q 20 parameters. At each position in the

Table 1 *S. cerevisiae* strains used in this study

Strain	Origin	Mating type	Description	Source
BC235	California Vineyard UCD 2120	*MAT***a**/*MATα*	*SPS2:EGFP:KanMX4/SPS2:EGFP:KanMX4*	Gerke *et al.* (2006)
BC239	California Vineyard UCD 2120	*MAT***a**/*MATα*	*SPS2:EGFP:NatMX4/SPS2:EGFP:NatMX4*	Gift of Barak Cohen
EC-33	Evolution Canyon Shady SF3, Israel	*MAT***a**/*MATα*	Initial isolate	Ezov *et al.* (2006)
YO795	EC-33	*MAT***a**	*gal7Δ0*::*KanMX4*, *SPS2:EGFP:NatMX4*, *hoΔ*::*HphMX6*	This study
YO1012	YO795	*MAT***a**	*gal7Δ0*::*KanMX4*, *SPS2:EGFP:NatMX4*, *hoΔ*::*HphMX6*, *ura3Δ0*	This study
YO1457–YO1459	YO1012	*MAT***a**	*gal7Δ0*::*KanMX4*, *SPS2:EGFP:NatMX4*, *hoΔ*::*HphMX6*, [*ura3Δ0*::*GAL80: URA3*]	This study
YPS163	Pennsylvania oak	*MATα*	*hoΔ*::*dsdAMX4*	Sniegowski *et al.* (2002)
YO796	YPS163	*MATα*	*gal7Δ0*::*KanMX4*, *SPS2:EGFP:NatMX4*, *hoΔ*::*dsdAMX4*	This study
YO964	YO796	*MATα*	*gal7Δ0*::*KanMX4*, *SPS2:EGFP:NatMX4*, *hoΔ*::*dsdAMX4*, *ura3Δ0*	This study
YO1454–YO1456	YO964	*MATα*	*gal7Δ0*::*KanMX4*, *SPS2:EGFP:NatMX4*, *hoΔ*::*dsdAMX4*, [*ura3Δ0*::*GAL80: URA3*]	This study
YO797	YO795 × YO796	*MAT***a**/*MATα*	*gal7Δ0*::*KanMX4*, *SPS2:EGFP:NatMX4*, *hoΔ*::*HphMX6*/*gal7Δ0*::*KanMX4*, *SPS2:EGFP:NatMX4*, *hoΔ*::*dsdAMX4*	This study
YPG3104	F_1 segregant of YO795 × YO796	*MAT***a**	Chromosome XIII disome for backcross *gal7Δ0*::*KanMX4*, *SPS2:EGFP:NatMX4*, *hoΔ*::*HphMX6*	This study
YO1014	YPG3104 × YO796	*MAT***a**/*MATα*	Diploid for chromosome XIII disome backcross	This study
YPG3121	F_1 segregant of YO795 × YO796	*MATα*	Chromosome XIII disome for backcross *gal7Δ0*::*KanMX4*, *SPS2:EGFP:NatMX4*, *hoΔ*::*HphMX6*	This study
YO1013	YO795 × YPG3121	*MAT***a**/*MATα*	Diploid for chromosome XIII disome backcross	This study
YPG3157	F_1 segregant of YO795 × YO796	*MAT***a**	Euploid strain for intercross *gal7Δ0*::*KanMX4*, *SPS2:EGFP:NatMX4*, *hoΔ*::*dsdAMX4*	This study
YPG3053	F_1 segregant of YO795 × YO796	*MATα*	Euploid strain for intercross *gal7Δ0*::*KanMX4*, *SPS2:EGFP:NatMX4*, *hoΔ*::*HphMX6*	This study
YO1640	YPG3157 × YPG3053	*MAT***a**/*MATα*	Diploid for euploid intercross	This study
YPG3140	F_1 segregant of YO795 × YO796	*MAT***a**	YPG3140 haploid *gal7Δ0*::*KanMX4*, *SPS2:EGFP:NatMX4*, *hoΔ*::*HphMX6*	This study
YO1650	YPG3140	*MAT***a**/*MATα*	YPG3140 diploid *ura3Δ0*/*ura3Δ0*	This study
YO2123	YO1650		YPG3140 haploid *ura3Δ0*	This study
YPG3161	F_1 segregant of YO795 × YO796	*MATα*	YPG3161 haploid *gal7Δ0*::*KanMX4*, *SPS2:EGFP:NatMX4*, *hoΔ*::*HphMX6*	This study
YO1652	YPG3161	*MAT***a**/*MATα*	YPG3161 diploid *ura3Δ0*/*ura3Δ0*	This study
YO2124	YO1652		YPG3161 haploid *ura3Δ0*	This study

reference genome, the most common base was identified for each strain, excluding insertions and deletions, and positions that differed between YO516 and YO528 were identified, allowing construction of a SNP table (Supporting Information, File S1).

Full genome sequencing of progenitor strains YO516 and YO528 resulted in poor uniquely mapping read coverage in the *HXT6* and *HXT7* loci due to the highly repetitive, AT-rich nature of the region. For strain YO528, the entire region was PCR-amplified using primers AO392 (5′-GTGCGGTCGGTAAAC AACTGAC-3′) and AO397 (5′-ATGCCCTCCGTGCCTTCATTG-3′), while, for strain YO516, three amplicons were amplified using primers AO392 with AO393 (5′-ACCATCCTTCGAGAT CCCCTG-3′), AO394 (5′-ACAGGGGATCTCGAAGGATGG-3′) with AO395 (5′-TGTACTACTGGCGGCGATTGG-3′), and AO396 (5′-ACCAATCGCCGCCAGTAGTAC-3′) with AO397. Regions were then sequenced by primer walking across the amplicons with Sanger sequencing (Beckman Coulter Genomics and Eurofins MWG Operon).

Progeny genotyping

RAD-seq was carried out (File S8) as described previously (Ludlow *et al.* 2013). For each lane of sequencing, raw read sequences were split into strain-specific pools based on their associated barcode sequence within the 5′ adaptor. Reads with unexpected strain barcodes or with barcodes having Phred [−10 log10 P(error)] quality scores <20 or ambiguous ("N") calls at any barcode base were discarded. Reads with more than two "N" calls in the body of the sequencing read were also discarded. The barcodes were then removed from the read sequences. Reads were aligned to the S288c reference (R64-1-1), and pileup files were generated as described above. The strain-specific read pools were then used to infer the genotypes of the progeny strains, also as above.

Other than at the *GAL7* locus, the genotype of the parental strain YO795 is assumed to be identical to its progenitor YO528, and parental strain YO796 is assumed to be identical to YO516. The bases called in the pileup files were compared to the YO516, YO528 SNP table and converted into parent 1 (YO796) or parent 2 (YO795) allele calls for the subset of positions polymorphic between the parents. At each such position in each strain, the frequency of P1-supporting reads was then compared to the frequency of P2-supporting reads. When the counts supporting one parental allele were at least 10-fold higher than the counts supporting the other parental allele, a final P1 or P2 allele assignment was made. Otherwise, the allele was defined as "mixed/heterozygous."

Marker quality filtering was then carried out, using only the 184 unselected progeny strains. Markers were removed unless they were called as P1 or P2 in at least 50% as many strains as the most frequently called marker and unless the ratio P1/(P1+P2) lay between 0.3 and 0.7. This defined a final set of 559 markers, and examination of the unselected strains genotyped at these markers using R/QTL (Broman *et al.* 2003) identified no obvious linkage between markers on different chromosomes or at distant positions on the same chromosome. The initial genotyping files for the sets of selected strains were filtered to include only this final set of markers, producing the final genotyping files.

Ploidy estimation

Ploidy estimation was carried out based on the proportion of all aligned reads aligning to each chromosome, calculated for each strain. Positions with only one aligned read were ignored. For each chromosome, coverage values were normalized using the median coverage for that chromosome from euploid strains YO795, YO796, and YO797 to give raw ploidy estimates. Under the assumption that most chromosomes are monosomic in each haploid strain, the raw estimates were then further normalized to take into account total genome size (which will be increased in aneuploid strains) by dividing each estimate by the median chromosomal ploidy estimate for that strain. Values were then rounded to the nearest whole number to give the final ploidy estimates. Normalized sequencing coverage plots (Figure 3B) were produced as described previously (Tan *et al.* 2013).

Identifying homozygous vs. heterozygous regions

For each strain, at each RAD-seq position, the counts of the P1- and P2-supporting reads were used to calculate a LOD score comparing the probability of the observed data under a heterozygous model *vs.* a homozygous (or haploid) model. The probability under the heterozygous model was calculated as the binomial probability of the observed counts assuming a probability of 0.5 for each allele. The probability under the homozygous model was calculated as the binomial probability of the observed counts assuming that the less frequent allele was an error with a probability of 0.01 with the more common allele having a probability of 0.99.

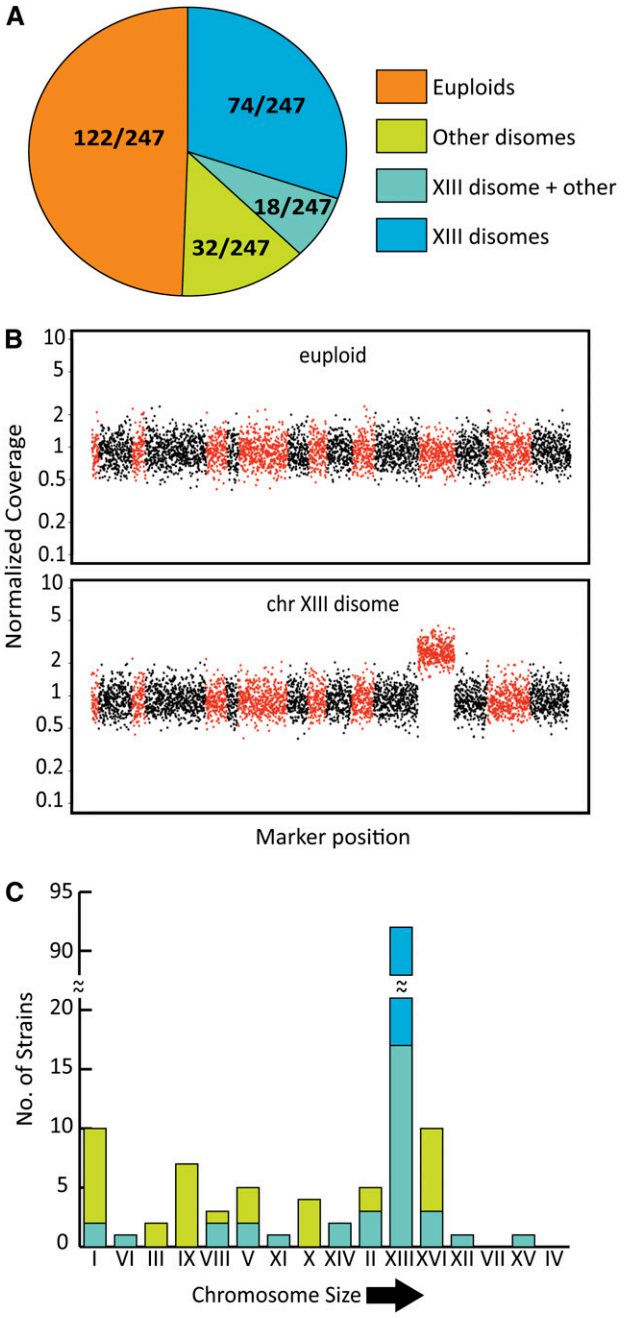

Figure 3 Frequency of aneuploidy among galactose-tolerant progeny. Ploidy estimates of the YO795 × YO796 galactose-tolerant progeny revealed that a large proportion of the strains were aneuploid. (A) Of the 247 strains sequenced, only 49% are euploid (orange) while 30% contain a chromosome XIII disomy (blue), 7% contain a chromosome XIII disomy with an additional chromosomal disomy (teal), and 13% contain a disomy other than chromosome XIII (green). (B) Plots of RAD-seq data show the ploidy of individual galactose-tolerant progeny. (C) The frequency of specific chromosomal aneuploidy among the progeny able to overcome galactose toxicity is shown ordered by chromosomal size. Color coding is the same as in A. Disomies of all chromosomes are represented except disomies of chromosomes VII and IV. Disomies of larger chromosomes such as chromosome XIII and chromosome XVI, which are present in multiple galactose-tolerant strains, are not present among a separately sequenced set of progeny grown on rich medium in the absence of galactose (see *Results*).

The final LOD score was calculated as Log_{10}[P(Hom)/P(Het)]. For strains with disomic chromosomes (see *Ploidy estimation*), markers on those chromosomes were called as heterozygous when their associated LOD score was below −3 and homozygous if their LOD score was >3. Homozygous markers were classified as homozygous P1 or homozygous P2 based on the most frequent allele count.

QTL mapping

In each cross except EC33-gal × YPG3121, markers on monosomic chromosomes were removed prior to mapping if they either lacked an allele call or had a mixed-allele call in 10% or more of the progeny strains. For disomic chromosomes, markers were removed prior to mapping only if they lacked an allele call in 10% or more of progeny strains. Because the EC33-gal × YPG312 cross contained fewer progeny, a more stringent threshold of 5% of strains was used to filter markers. QTL mapping was done by comparing the P1 and P2 allele frequencies at each marker, across the set of strains, to a null hypothesis of 1:1 segregation, using the binomial exact test (two-sided) implemented in R (R Development Core Team 2013). In each analysis, Bonferroni correction for the number of markers tested was applied to an initial significance threshold of $P = 0.05$, setting a final significance threshold.

Testing for biased allele segregation in backcrosses with disomic strains

For each backcross involving a strain disomic for chromosome XIII, each marker on that chromosome was characterized as heterozygous, homozygous P1, or homozygous P2, as above. For each of these markers, a null model of random allele/chromatid segregation was generated using formulas for trivalent pairing with centromere linkage (Koller *et al.* 1996) with physical distance from the centromere used as a proxy for linkage based on 0.0038 crossovers per kilobase on chromosome XIII (Mancera *et al.* 2008). The observed allele pattern (heterozygous, homozygous P1, homozygous P2) frequencies across the progeny strains were then compared to this model using the multinomial exact test implemented in R. Bonferroni correction for the number of markers tested was applied to an initial significance threshold of $P = 0.05$, setting a final significance threshold. Markers fixed in the backcrosses were not counted for correction and were assigned a *P*-value of 1. Note that QTL mapping on disomic chromosome XIII was not carried out on progeny of the original cross due to the very low levels of crossing over associated with generation of the disomy.

Results

A FACS-based method for extreme QTL mapping

FACS-QTL integrates fluorescence-based sorting of tetrads with highly multiplexed genotyping of individual recombinant progeny that overcome extreme phenotypic selections. The method simplifies the isolation of large numbers of progeny by replacing the auxotrophic markers commonly used in BSA methods (Ehrenreich *et al.* 2010; Parts *et al.* 2011) with a single FACS sorting step (Figure 1) enabled by the integration of the sporulation-specific reporter *SPS2-GFP* at the *SPS2* locus in both parental strains (*Materials and Methods*). Because *SPS2-GFP* expression begins early in meiosis (Coluccio *et al.* 2004; Gerke *et al.* 2006), the fluorescent population includes tetrads, dyads, and incompletely formed spores. However, restrictive FACS gating can select fully formed tetrads away from these other cells (Ludlow *et al.* 2013), permitting the isolation of large numbers of tetrads even in crosses with low sporulation efficiencies. In this study, we were able to rapidly isolate $>10^6$ tetrads from a cross with a 20% sporulation efficiency to yield >99% recombinant haploid progeny (File S2). After sorting, the tetrads were disrupted, and the resulting population of haploid progeny was grown on plates with selection as well as a no-selection control plate, which was used to calculate the proportion of spores that survive the selection (*Materials and Methods*). Because spores are plated directly on the selective medium, each colony that survives the selection represents a unique meiotic product that can be individually genotyped for QTL mapping and molecular karyotyping. In this study, we used a multiplexed RAD-seq protocol (Baird *et al.* 2008) that sequences the same ∼3% of each segregant's genome, providing a set of genetic markers distributed across all of the chromosomes (Lorenz and Cohen 2012). However, FACS-QTL is also compatible with a variety of other genotyping methods, including whole-genome sequencing.

Suppression of galactose toxicity

We chose to study the galactose-dependent toxicity resulting from a *GAL7* deletion (*gal7*Δ) as a monogenic trait for three reasons. First, the metabolic and regulatory networks of galactose utilization are one of the best-characterized systems in yeast. Second, yeast *gal7*Δ mutants are an established model for the monogenic trait classic galactosemia in humans, which is caused by accumulation of the same toxic intermediates (Fridovich-Keil and Jinks-Robertson 1993; Mehta *et al.* 1999). Third, the toxic effects of even small concentrations of galactose on *gal7*Δ strains impose a stringent growth selection, allowing the genetic architecture of the extreme tail of the galactose-tolerant population to be investigated by FACS-QTL. Our working hypothesis was that FACS-QTL would allow us to isolate and characterize rare individuals that could overcome the galactose toxicity and that these individuals would possess a complex combination of alleles capable of suppressing the monogenic trait.

We began our investigation of galactose toxicity by selecting two parental strains from a collection of genetically diverse natural variants of *S. cerevisiae* (Cromie *et al.* 2013). To avoid the presence of uninformative alleles that might confound the selection, *e.g.*, galactose transporter loss-of-function alleles, we chose two strains that were initially able to metabolize galactose (Table S1). EC-33 was isolated from

Table 2 Strain doubling times with standard errors in increasing concentrations of galactose in the presence of raffinose and antimycin A

	0% Galactose	0.01% Galactose	0.05% Galactose	0.1% Galactose
EC-33	169 ± 1 min	172 ± 3 min	170 ± 4 min	165 ± 2 min
EC33-gal	181 ± 2 min	223 ± 7 min	No growth	No growth
YPS163	263 ± 15 min	249 ± 7 min	262 ± 18 min	184 ± 3 min
YPS163-gal	222 ± 3 min	634 ± 45 min	No growth	No growth
EC33-gal × YPS163-gal	159 ± 10 min	271 ± 20 min	No growth	No growth

Evolution Canyon (Ezov *et al.* 2006; Katz Ezov *et al.* 2010), and YPS163 was isolated from soil at the base of an oak tree in Pennsylvania (Sniegowski *et al.* 2002). These strains have an average sequence divergence of 4.2 polymorphisms per kilobase (Cromie *et al.* 2013). To confer the galactose toxicity phenotype, we deleted *GAL7* from haploid, monosporic derivatives of both strains, producing strains YO795 (hereafter EC33-gal) and YO796 (hereafter YPS163-gal), and confirmed that the mutation rendered them unable to grow on rich medium containing 2% galactose in the presence of the respiratory inhibitor antimycin A, which prevents alternative carbon source utilization (Donnini *et al.* 1992; Ko *et al.* 1993) (Table S1).

To assay the strength of galactose toxicity, we measured growth of the *gal7*Δ haploid parental strains, and the heterozygous diploid strain generated by mating them, on several concentrations of galactose ranging from 0.01 to 0.1% in the presence of 2% raffinose and 1 μg/ml antimycin A (Table 2). Then, to choose a sufficiently stringent selection, we tested the ability of individual progeny of the cross (generated by FACS-QTL) to grow on the same galactose-containing media. Consistent with the presence of phenotypic heterogeneity in the cross, the proportion of progeny strains surviving the selection decreased with increasing galactose concentration (Table 3). Based on these experiments, we chose a final galactose concentration (0.05%) on which neither the *gal7*Δ parental strains nor the heterozygous diploid were able to grow as single cells, but on which recombinant progeny (at a frequency of ∼1/1000) were able to form colonies after 2 days. At this concentration, galactose toxicity behaves as a monogenic trait with 99.9% of the progeny suffering loss of viability due to the *gal7*Δ mutation. The low frequency of progeny overcoming selection is consistent with a highly complex, unique genetic solution, *e.g.*, the segregation of 9–10 independent loci.

To characterize the rare genotypes capable of suppressing *gal7*Δ-dependent galactose toxicity, we used RAD-seq to individually genotype 247 galactose-tolerant progeny of the EC33-gal × YPS163-gal cross at 469 loci (*Materials and Methods*). In addition to providing a set of genotyping markers, RAD-seq can be used to detect aneuploidy based on relative sequencing coverage across each chromosome (Tan *et al.* 2013). Individual RAD-seq analysis of the 247 galactose-tolerant progeny from our cross revealed a surprisingly high degree of aneuploidy (File S3) with more than half of the strains harboring at least one extra chromosome (Figure 3A). The availability of individual genotypes of the selected individuals allowed us to test whether the euploid and aneuploid subpopulations had arrived at distinct solutions to the selective pressure of galactose toxicity. To perform this analysis, we mapped QTL separately in the two major subpopulations: the euploid strains and the strains with a single disomy of the most frequently aneuploid chromosome (XIII). In both subpopulations, we identified markers significantly associated with selection based on a binomial *P*-value of $<10^{-4}$ ($P < 0.05$ with Bonferroni correction for ∼500 markers) for a null model of 50:50 allele segregation.

Euploid subpopulation harbors QTL containing GAL3, GAL80, and HXT3/6/7

Linkage analysis in the subpopulation of euploid segregants identified three major QTL peaks for galactose tolerance (Figure 4A and Figure S1). Peak 1, selected from the EC33-gal parent, spans a region on chromosome IV containing the signal transducer of the galactose pathway *GAL3* (Torchia and Hopper 1986; Lohr *et al.* 1995). Peak 3, selected from the YPS163-gal parent, spans a region on chromosome XIII that includes the *GAL80* locus, a transcriptional repressor of numerous genes in the galactose utilization pathway (Figure 2) (Nogi *et al.* 1977; Johnston 1987). Both candidate genes were within a 1.5-$\log_{10}$ *P*-value drop from the peak maximum (File S4). The central regulatory roles of these two genes in galactose metabolism (Figure 2) are well established, and the two proteins are known to physically interact (Johnston 1987; Egriboz *et al.* 2011). The presence of multiple single nucleotide polymorphisms (SNPs) within the loci (Figure 5 and File S1) further supported *GAL3* and *GAL80* as strong candidate genes within the regions. The final QTL in our euploid segregants, peak 2, spanned a region on chromosome IV that is genetically unlinked to QTL peak 1 on the same chromosome (∼620 kb or ∼250 cM apart). Peak 2 includes the tandemly oriented hexose transporters *HXT3*, *HXT6*, and *HXT7*, which are within a 1.5-$\log_{10}$ *P*-value drop from the QTL peak maximum. The sequence of the *HXT6/7* region in both parents differed substantially from that of the reference strain (Figure 5 and File S5). The selected allele, derived from YPS163-gal, contained numerous amino acid changes in the coding sequences of *HXT3*, *HXT6*, and *HXT7*, relative to the reference strain S288c, as well as multiple SNPs within promoter regions. The unselected allele, derived from EC33-gal, contained an *HXT3* locus identical to that of the reference strain and a chimeric *HXT6*/7, similar to a previously observed allele (Liang and Gaber 1996), which fuses the *HXT6* promoter region [identical to the

Table 3 Concentration of galactose determines frequency of galactose-tolerant progeny

Description	% Galactose	No. of spores/plate	No. of galactose-tolerant spores/plate	Frequency of galactose-tolerant progeny
EC33-gal × YPS163-gal	0.1	2.7×10^5	21	$1/(1 \times 10^4)$
EC33-gal × YPS163-gal	0.05	2.7×10^5	230	1/1000
EC33-gal × YPS163-gal	0.02	2.7×10^5	4400	1/60

reference (S288c) *HXT6* promoter] to the *HXT7* coding region. As the galactose pathway is induced by intracellular galactose, it is possible that one, or more, of these HXT transporters is important for the initial entry of galactose into the cell (Donnini *et al.* 1992; Boles and Hollenberg 1997; Reifenberger *et al.* 1997; Wieczorke *et al.* 1999), leading to expression of *GAL* pathway genes including the major galactose transporter *GAL2*. Together, the *GAL80*, *GAL3*, and *HXT* loci indicate that combinations of alleles in genes that govern the regulation of galactose utilization, rather than genes that encode enzymatic functions for either the catabolism of galactose or the degradation of its toxic intermediates, contribute to the most frequent euploid genotypes allowing galactose tolerance in our cross.

A nongenetic component contributes to galactose tolerance of the euploid segregants

The identification of only three loci in the galactose-tolerant euploid strain population was inconsistent with the low frequency of galactose-tolerant progeny in the population. In a cross between two haploid yeast strains, three unlinked loci cosegregate with a frequency of 1 in 8 recombinant progeny. The fact that only ~1 in 1000 of the strains with this genotype actually survived the phenotypic selection suggests the contribution of additional factors. One possible explanation is that the euploid survivors represent a highly heterogeneous set of complex genetic solutions; *i.e.*, the three loci plus several combinations of a variety of other alleles are needed to overcome the selection. To test whether additional loci were segregating through the cross, we applied the selection to an intercross between two F_1 euploid progeny (Table 4), thereby fixing all three previously identified QTL. The resulting 1/72 frequency (18/1300) of galactose-tolerant progeny suggested that either many more QTL were still segregating through the cross or there was a nongenetic component to the phenotype. To test for nongenetic effects, we chose two galactose-tolerant euploid segregants from our initial cross and converted them to homozygous diploids by transient expression of the gene encoding the HO endonuclease (*Materials and Methods*). The resulting self-mated diploids, YO1650 and YO1652, were sporulated, and individual haploid spores (isogenic at all loci except for the mating-type locus) were plated on galactose by both hand dissection of tetrads and FACS-QTL. As the progeny of these self-matings are genetically identical to each other and their galactose-tolerant parents, in the absence of nongenetic effects, 100% of the progeny should be galactose-tolerant. In contrast, we observed a 7–18% survival rate on selection of the isogenic progeny (Table 4 and Table S2). These results support the involvement of a nongenetic event in the galactose-tolerant phenotype of the two original euploid strains, possibly deriving from cell-to-cell differences in intracellular protein or transporter levels (Acar *et al.* 2005; Kar *et al.* 2014). We further found that single cells from clonal populations of galactose-tolerant progeny also demonstrated low survival rates when grown on galactose medium, suggesting that this nongenetic event could affect mitotically dividing cells as well as germinating spores (Table S2).

High frequency of aneuploidy among galactose-tolerant segregants

The remaining galactose-resistant progeny were aneuploids that harbored an extra copy of at least one chromosome. Interestingly, the majority of these (74% of the aneuploid class and 38% of all selected progeny) harbored an extra copy of chromosome XIII (Figure 3A and File S3). The isolation of such a large number of XIII disomes was significant for two reasons. First, one of our major QTL, containing the *GAL80* gene, resides on chromosome XIII. Second, additional copies of chromosome XIII specifically have been shown to be poorly tolerated (if not lethal) in several studies of aneuploidy using a variety of methods and strain backgrounds (Torres *et al.* 2007; Tan *et al.* 2013). These results suggest that some aspect of chromosome XIII aneuploidy might provide a strong selective advantage for cells in response to *gal7*Δ-dependent galactose toxicity, perhaps via overexpression of specific genes, such as *GAL80*.

To test whether some aspect of the FACS-QTL method was itself producing high levels of aneuploidy, we isolated recombinant progeny from the EC33-gal × YPS163-gal cross by manual tetrad dissection onto nonselective medium (YPD) and examined their molecular karyotype by RAD-seq (File S6). Among 46 manually dissected tetrads, four produced only two viable spores with either chromosome I or IX disomies, and one tetrad produced only one viable spore containing disomies of chromosome III and chromosome VIII. This frequency of meiotic chromosome missegregation (~1 in 10 meiotic events) is approximately two orders of magnitude higher than rates that have been previously measured in a different strain background (Sora *et al.* 1982). However, the frequency of disomes (9/145 strains) among the unselected segregants was still much lower than that observed among our selected segregants (125/247 strains), and we noted that none of the unselected, hand-dissected segregants contained

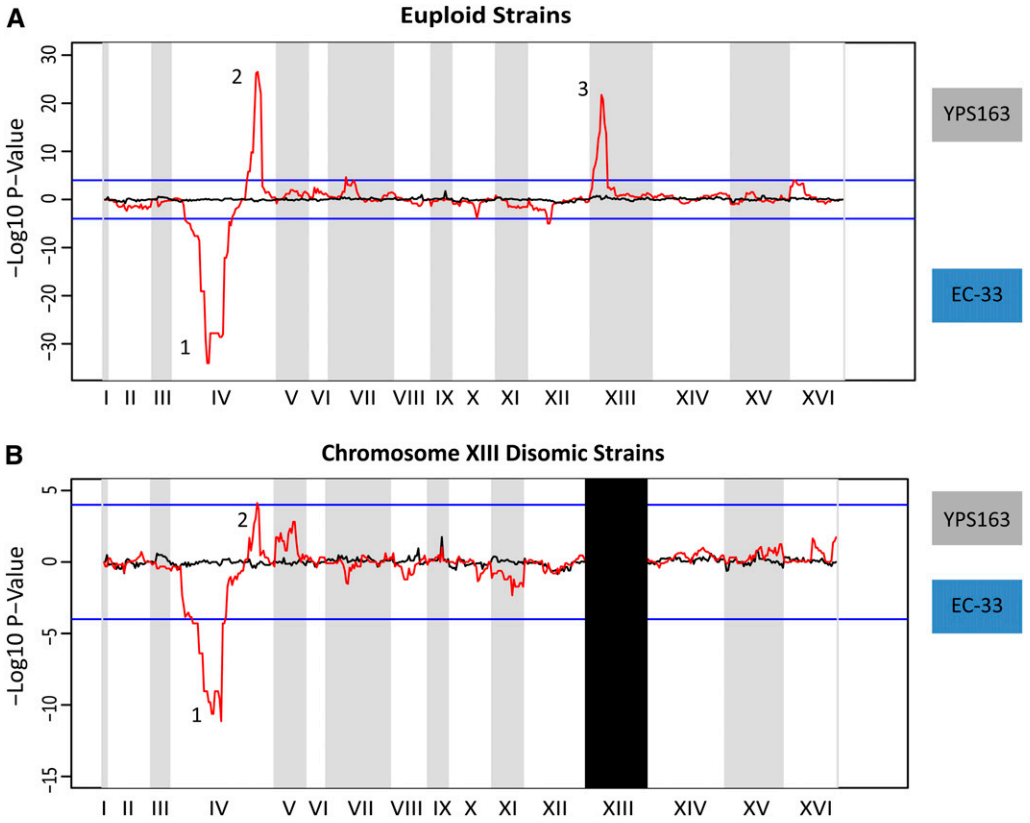

Figure 4 QTL mapping of two classes of galactose-tolerant progeny. Observed allele frequencies at each marker were compared to an expected 1:1 allele segregation frequency among all (unselected) progeny by binomial exact test with selected populations in red and the unselected population in black. QTL peaks indicating the overrepresentation of alleles from the YPS163-gal parent are shown above the upper blue line while peaks indicating the overrepresentation of markers from the EC33-gal parent are shown below the lower blue line. Blue lines denote a significance threshold of *P*-value = 10^{-4} (nominal 0.05 with Bonferonni correction). (A) QTL mapping identified three significant QTL peaks among euploid galactose-tolerant strains (red). On chromosome IV, peak 1 indicates an enrichment of the EC-33 region containing the *GAL3* gene and peak 2 indicates the YPS163 region containing *HXT3/6/7*. On chromosome XIII, peak 3 indicates an enrichment of the region containing the YPS163 *GAL80* allele. Examination of the haplotypes of the galactose-tolerant euploid strains indicated how strongly the three regions were selected. One hundred twenty-one of 122 strains inherited the EC-33 allele of *GAL3*, 117/122 strains inherited the YPS163 alleles of *HXT3*, *-6*, and *-7*, and 111/122 strains inherited the YPS163 allele of *GAL80* or had crossovers between the RAD markers flanking these loci. (B) QTL mapping of selected chromosome XIII disomic galactose-tolerant progeny (red) identified two of the same genomic regions as the euploid strains (peak 1 and 2) although with reduced significance. The chromosomal disomy in these strains precluded QTL mapping on chromosome XIII.

a chromosome XIII disomy, the most frequent disomy among our selected progeny.

Disomic spores can arise as a result of chromosome nondisjunction during either the first or the second meiotic divisions. Disomies can also arise by mitotic missegregation soon after spore germination, but the heterozygosity of our disomic chromosomes argues against such a mitotic event. The segregation patterns of centromere-linked markers are a signature that can be used to distinguish between the two meiotic possibilities. Meiosis I missegregation events result in centromeric heterozygosity, while meiosis II events (or mitotic events) result in centromeric homozygosity. Centromere-linked markers on the disomic chromosomes from both the FACS-QTL-selected and hand-dissected unselected populations were heterozygous in the vast majority of cases (File S2 and File S3), indicating that the disomies had arisen due to meiosis I missegregation events, with these events occurring at a relatively high frequency in this cross.

Chromosome XIII disomy is an essential component of galactose tolerance in disomic strains

The large proportion of galactose-tolerant segregants harboring a chromosome XIII disomy suggested that an extra copy of that chromosome was beneficial for survival on galactose in the *gal7*Δ background. To test whether chromosome XIII disomy was necessary for galactose tolerance in these strains, we applied our sorting method to backcrosses between each parent (EC33-gal and YPS163-gal) and an F_1 strain of the opposite mating type that was disomic for chromosome XIII (YPG3121 or YPG3104). In crosses between euploid and disomic strains, disomy segregates 2:2 (St. Charles *et al.* 2010). We sequenced 45 galactose-tolerant progeny from the cross EC33-gal × YPG3121 (414 markers) and 86 progeny from the cross YPS163-gal × YPG3104 (420 markers) and observed that, in contrast to the expected 50% random segregation of the disome, the vast majority (129/131) of the galactose-tolerant progeny from the backcrosses were disomic (File S7). These results are consistent with our hypothesis that chromosome XIII disomy contributes to galactose tolerance in these strains.

One possible explanation for the selective advantage conferred by the chromosome XIII disomy is that it increases the expression level of one or more genes on that chromosome that are important for galactose tolerance. Overexpression of *GAL80* was a strong candidate because overexpression of the Gal80p transcriptional repressor is known to reduce expression levels of genes in the galactose pathway (Nogi *et al.* 1984), an effect that should reduce

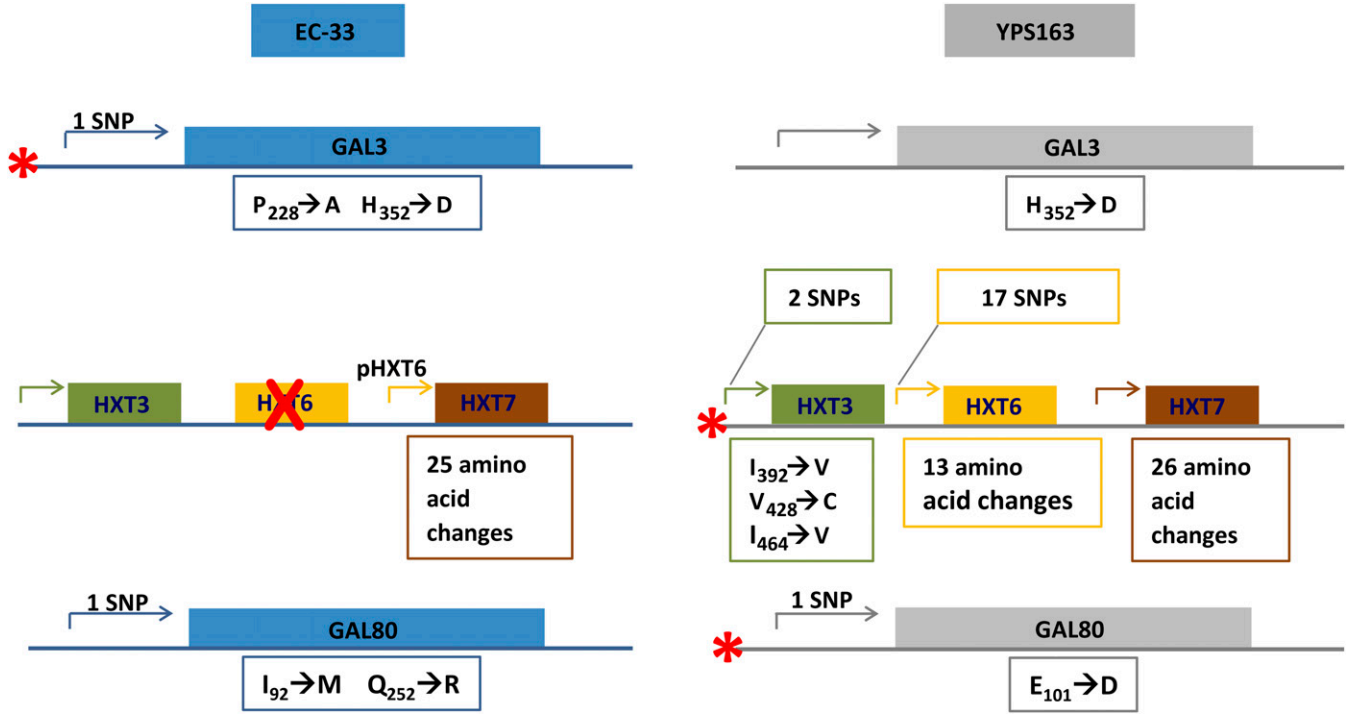

Figure 5 Polymorphisms within candidate genes. Natural variant strains EC-33 (blue) and YPS163 (gray) each have multiple SNPs, as compared to the reference strain S288c, within the three candidate genes/gene clusters associated with galactose tolerance. SNPs in the promoter regions and missense SNPs within each ORF (boxes under each allele) are indicated for each gene (see File S1, File S2, and File S5 for sequencing results). For each gene/gene cluster, the allele enriched in galactose-tolerant progeny of the EC33-gal × YPS163-gal cross is denoted with a red asterisk. While the coding regions of *HXT7* of both strains contain near identical changes compared to the reference strain, the selected version (YPS163) maintains the *HXT7* promoter while the unselected allele is a chimeric fusion of the *HXT7*-coding sequence with the *HXT6* promoter. The YPS163 *HXT6* and *HXT3* regions have variation in their promoter and coding regions compared to S288c while the EC-33 *HXT6*-coding region is absent and the *HXT3* gene is identical to the reference strain.

galactose toxicity in our strains (Figure 2). To test this hypothesis, we first attempted deleting one copy of *GAL80* in the disomic strain, thereby restoring *GAL80* copy number in the context of an otherwise aneuploid strain. Unfortunately, numerous attempts [including a variety of different strains, markers (hph-NT1 and URA3MX4), and transformation conditions] failed to yield transformants with the desired deletion. As an alternative approach, we increased the copy number of *GAL80* in both the euploid EC33-gal and YPS163-gal parents by integrating a second copy of the gene (the well-characterized S288c allele) under its native promoter. Spotting assays (Figure S2) demonstrated that an extra copy of *GAL80* relieved the toxicity of 0.05% galactose in both parental strains.

Selected alleles and an aneuploidy–allele interaction contribute to galactose resistance of the chromosome XIII disomic strains

To assess the contribution of genetic loci in the aneuploid strains, we performed two sets of analyses. First, we mapped QTL in the subpopulation of the original cross that contained only a chromosome XIII disome, excluding any markers on chromosome XIII itself. Second, we mapped QTL in backcrosses between two of these disomic progeny and the parental strains (above).

QTL mapping in the disomic population from the original cross identified two significant peaks that corresponded to the same positions as the two chromosome IV peaks observed in the euploid population, *i.e.*, the regions containing the *GAL3* and *HXT* loci (Figure 4B and Figure S1). However, while most of the disomic strains (64/73) inherited either the EC33-gal allele of *GAL3* or had a crossover between the RAD markers flanking the *GAL3* locus, selection for the *HXT* loci (53/73) was much less strong.

The two progeny strains used in the backcrosses possessed the favored alleles at both the *GAL3* and *HXT* loci. Therefore, the *GAL3* locus was fixed in the backcross to EC33-gal and the *HXT* locus was fixed in the backcross to YPS163-gal (Figure 4B and Figure S1). In the backcross between YPS163-gal and YPG3104, fixed for the *HXT* alleles, we expected 25% of backcross progeny (those that inherited the *GAL3* locus and the extra copy of chromosome XIII) to display galactose tolerance. The resulting frequency of 20% galactose-tolerant segregants from this backcross (Table 4) was consistent with this expectation, and sequencing of the galactose-tolerant progeny confirmed selection for the *GAL3* region and the disomy (Figure S3 and File S7). In the backcross between EC33-gal × YPG3121, the *GAL3* locus was fixed, and the 25% frequency of galactose-tolerant progeny suggested that the disomy was segregating along

Table 4 Frequencies of galactose-tolerant progeny using FACS-QTL method

Description	Cross	No. of spores/plate	No. of galactose-tolerant spores/plate	Frequency of galactose-tolerant progeny
EC33-gal × YPS163-gal	YO795 × YO796	4×10^4	72	1/540
EC33-gal × chromosome XIII disome	YO795 × YPG3121	470	108	1/4
Chromosome XIII disome × YPS163-gal	YPG3104 × YO796	414	78	1/5
Euploid intercross	YPG3157 × YPG3053	1300	18	1/72
Euploid homozygous diploid	YPG3161 diploid	627	42	1/15
Euploid homozygous diploid	YPG3140 diploid	631	63	1/10

with one other allele, presumably the unfixed *HXT* locus. Sequencing of the galactose-tolerant progeny confirmed selection for the disomy, and the most prominent QTL peak was at the *HXT* locus, falling just below the significance threshold (Figure S3 and File S7). Taken together, QTL mapping results from the original cross and the backcrosses suggest that the loci containing *GAL3* and the *HXT* genes contribute to the galactose tolerance of both the euploid and aneuploid strains.

Closer analysis of the galactose-tolerant progeny of the EC33-gal × YPG3121 cross indicated an additional bias in the alleles observed in the region of (disomic) chromosome XIII containing the *GAL80* locus. This region is heterozygous in YPG3121, and random segregation of alleles unlinked to the centromere (Koller *et al.* 1996) predicts that, among our disomic spores, ~50% should be homozygous for the EC33-gal allele (the disfavored allele of *GAL80* in the selected euploid population). Instead, only 7/45 (16%) strains were homozygous for the EC33-gal allele of the marker closest to *GAL80*. No significant difference from the null model was seen in other regions of chromosome XIII, including other regions that are heterozygous in YPG3121 (Figure 6A). In contrast, in the YPS163-gal × YPG3104 backcross, there appeared to be no bias in the inheritance of alleles in the *GAL80* region or in any other region of chromosome XIII (Figure 6B). In this backcross, the two major subpopulations of progeny are heterozygous for *GAL80* or homozygous for the allele of *GAL80* favored in the selected euploid population. In summary, two backcrosses using disomic strains indicated that disomy of chromosome XIII was necessary, but insufficient, for galactose tolerance. Instead, a biased allele segregation pattern was seen in a region encompassing *GAL80*, so that at least one copy of the *GAL80* allele selected in the euploid subpopulation was present in galactose-tolerant strains disomic for chromosome XIII.

Model for galactose tolerance

Taken together, our results suggest the following model for galactose tolerance in the *gal7*Δ background. In the cross between our galactose-sensitive parents (EC33-gal and YPS163-gal), 0.1% of the recombinant progeny were able to survive the stringent selection imposed by the addition of 0.05% galactose. These progeny fell into two classes with approximately equal frequencies: euploids and aneuploids (the majority of which harbored an extra copy of chromosome XIII). The euploid population contained three major QTL peaks encompassing the *GAL3*, *GAL80*, and *HXT3/6/7* loci. However, the fact that galactose tolerance is exhibited by only ~10% of progeny derived by self-mating euploid, galactose-tolerant strains suggests 10% penetrance of the resistant genotype in the euploid subpopulation. The discrepancy between the actual frequency of tolerant euploid progeny, given this level of penetrance (~0.5% = 50% euploid resistant progeny * 0.1% total resistant progeny/10% penetrance) and the predicted frequency based on the segregation of only three loci, suggests that genetic factors remain unexplained in this subpopulation. In the aneuploid subpopulation, results from backcrosses support the model that galactose tolerance is explained by major-effect QTL spanning the *GAL3* and *HXT* loci and a chromosome XIII disomy that includes at least one copy of the euploid-selected (YPS163) *GAL80* allele, *i.e.*, an aneuploidy–allele interaction. The heterozygosity of the centromere-linked markers (in the original cross) supports the hypothesis that the extra copy of chromosome XIII, and thus the additional copies of *GAL80*, arise from events in meiosis, specifically meiosis I nondisjunction, which occurs in this cross orders of magnitude more frequently than has been reported for other strain backgrounds.

Discussion

In this study, we present a method, FACS-QTL, for linkage-based QTL mapping in yeast that combines isolation of large numbers of yeast progeny under extreme selection with genotyping of individual segregants by partial genome sequencing. The method involves minimal strain engineering, requiring only the introduction of a sporulation-specific reporter, and provides a quick and simple way to generate and individually genotype (and karyotype) large numbers of prototrophic progeny from any yeast cross. Direct comparison of BSA methods with sequencing of individual progeny (Wilkening *et al.* 2013) suggests that our method should capture many of the strengths of BSA approaches while avoiding potential pitfalls of pooling progeny, such as mutational sweeps and subpopulations that have undergone ploidy changes. FACS-QTL is designed to characterize large numbers of individuals isolated by selection from extreme tails of phenotypic variation. This makes it particularly well suited for use in models of human monogenic diseases, where knowledge of rare genotypes that modify the underlying disease allele could provide new avenues for therapeutic

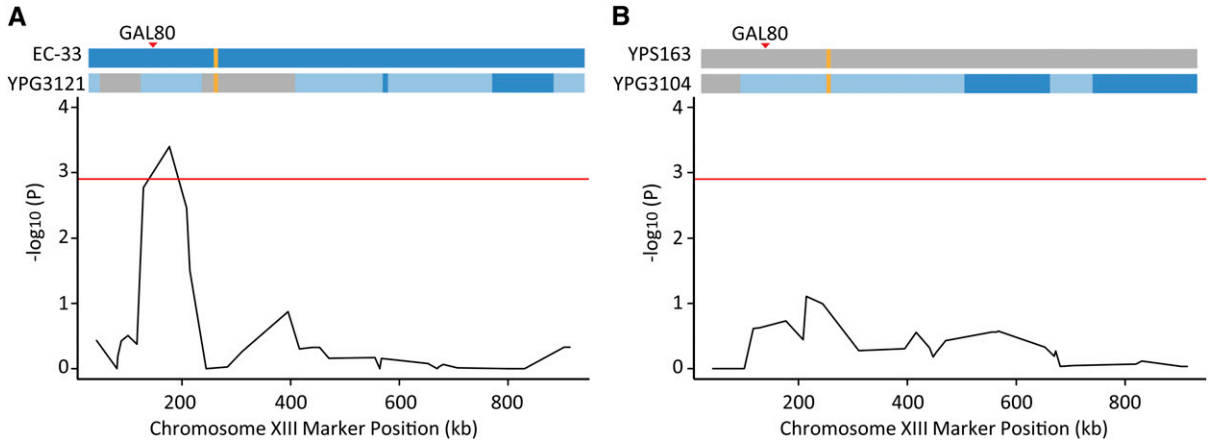

Figure 6 Biased segregation of the *GAL80* region in galactose-tolerant progeny of backcrosses between F_1 chromosome XIII disomic progeny and original parent strains. Essentially all progeny of the backcrosses were disomic for chromosome XIII. Among these disomic progeny, each marker was scored as heterozygous, homozygous EC-33, or homozygous YPS163. Observed frequencies of these classes across each set of backcross progeny were compared to a null model of random homolog segregation in meiosis I, using the multinomial exact test. The haplotypes, as inferred from marker sequencing, of both parents in each backcross are indicated above the plots: dark blue, EC33-gal parent; gray, YPS163-gal parent; light blue, heterozygous; and orange, chromosome XIII centromere location. (A) EC33-gal × YPG3121 galactose-tolerant F_1 strain shows nonrandom segregation in regions surrounding the *GAL80* allele with a larger-than-predicted number of progeny being heterozygous and fewer being homozygous for the EC-33 allele. (B) All chromosome XIII markers of YPG3104 × YPS163-gal progeny segregate in agreement with the null model. Comparison of the two backcrosses indicates that at least one copy of the YPS163 *GAL80* allele is selected in galactose-tolerant progeny with a chromosome XIII disomy, suggesting an aneuploidy–allele interaction.

intervention (Antonarakis and Beckmann 2006; Brinkman *et al.* 2006; Cutting 2010).

Applying our method to a yeast model for a human monogenic disease, classic galactosemia, allowed us to explore the mechanisms by which a monogenic trait can be ameliorated. The set of rare galactose-tolerant progeny that we obtained from our yeast cross can be split into two major classes: a set of strains where disomy of chromosome XIII is necessary for galactose tolerance and a group of euploid strains whose galactose tolerance is independent of this mechanism but requires a rare nongenetic event. Both of our major subpopulations were characterized by a selected genotype along with an additional factor, a nongenetic event in the euploid strains and chromosome missegregation in the chromosome XIII disomes. Neither group of strains displayed a single, purely allele-based, solution to galactose selection. Such a solution may exist in our cross, but involving such a large number of loci that it is even more rare than the two major solutions that we observed, and as such, the progeny that we have isolated are likely to represent the most frequent, "easily accessed" solutions. It is also possible that, in a different genetic background, a purely allele-based solution might be more accessible. Taken as a whole, our results indicate that the rare mechanisms by which the phenotypes of monogenic traits can be modified are likely to be highly heterogeneous.

The low frequency of galactose-tolerant progeny obtained by self-crossing two galactose-tolerant euploid strains indicated a nongenetic component in the phenotypes of the euploid subpopulation. Therefore, it appears that this subpopulation is best explained by selected alleles at three loci relevant to *GAL* pathway regulation, along with a rare nongenetic event, giving rise to a galactose-tolerant phenotype. In the absence of glucose, expression of genes in the *GAL* pathway is induced by the presence of galactose. Failure to induce these genes should allow *gal7Δ0* strains to remain viable in the presence of galactose (Bhat 2008). We hypothesize that the selected genotypes position strains close to the *GAL* pathway induction threshold such that a stochastic, nongenetic event can push some strains below the threshold into the uninduced state and confer galactose tolerance. Switching between these two states has been observed at similar concentrations of galactose in *GAL80* loop knockout strains (strains constitutively expressing *GAL80*) in which the rate of switching between the two states depended on Gal80p levels and galactose concentration (Acar *et al.* 2005).

Similar to the euploid subpopulation, the galactose-resistant subpopulation of chromosome XIII disomes in our cross appears to be characterized by selected alleles at two loci relevant to *GAL* pathway regulation along with an additional rare event, in this case the missegregation of chromosome XIII. In microorganisms such as *S. cerevisiae*, which are capable of producing large populations of individuals, rare cases of chromosomal missegregation can provide the population with the genetic variation required for rapid adaptation to new challenges within the environment (Chen *et al.* 2012; Yona *et al.* 2012). Aneuploidy occurring due to rare mitotic chromosome missegregation events has been shown to provide a mechanism for rapid adaptation in times of stress by driving large phenotypic changes through the simultaneous increase in copy number of multiple genes relevant to the trait under selection (Rancati *et al.* 2008; Yona *et al.* 2012; Tan *et al.* 2013). Compared to mutational

events, particularly multiple mutational events, aneuploidy occurs at a relatively high rate, providing a more accessible mechanism of adaptation and one that is also more easily reversed if environmental conditions change.

In general, increases in gene copy number lead to a corresponding increase in protein levels (Pavelka *et al.* 2010). We expect, therefore, that an extra copy of a chromosome will increase the relative protein abundance of most genes encoded on that chromosome. Aneuploidy can, however, also result in a cascade of expression-level effects across the genome. For example, in a disome, even modest increases in the expression of some genes, such as transcription factors, present on the disomic chromosome, can have attenuated effects on transcription levels of related pathway genes found on other chromosomes (Rancati *et al.* 2008). Increasing the expression of a subset of the genome in this way has costs, including creating stoichiometric imbalances in protein complexes, triggering of stress response genes, and causing cell cycle delays (Torres *et al.* 2007; Thorburn *et al.* 2013). For aneuploid cells growing in environments facing little selective pressure, these effects can greatly impact their relative fitness. So, while aneuploids within a population may be uniquely equipped to respond to unexpected, dramatic shifts in surrounding conditions, they represent solutions to selection that may also be reversed when selective pressures are removed or more stable genetic adaptation occurs over time (Yona *et al.* 2012).

One example of a dramatic change in environment occurs when pathogenic microorganisms are exposed to drugs for treatment of infection. In these circumstances, aneuploidy generated during mitosis is frequently observed as a mechanism underlying increased virulence and the development of drug resistance (Selmecki *et al.* 2006, 2009; Polakova *et al.* 2009; Sionov *et al.* 2010). In addition, recent work elucidating the sexual cycles of various fungal pathogens has revealed large numbers of aneuploid progeny where missegregation appears to occur during meiosis. The observed aneuploidy is linked to phenotypic changes such as increased resistance to drugs and suggests a tolerance for missegregation during meiosis as an effective evolutionary strategy (Reedy *et al.* 2009; Ni *et al.* 2013). Thus, targeting aneuploidy may prove an effective approach in the development of new antifungal drugs.

In our cross, an exceptionally high rate of aneuploidy arose from meiosis I nondisjunction events even in the absence of selection. This suggests a significant defect in the machinery of meiotic chromosomal segregation or recombination, presumably leading to some reduction in fitness. However, in the case of galactose toxicity, tolerance of high levels of meiotic missegregation has also provided the population with easily accessible solutions to a strong selective pressure. In natural variant strains that are exposed to unexpected fluctuating environmental conditions, such a lack of fidelity could serve as a bet-hedging mechanism as cells transition from a state of dormancy to actively competing for resources within an untested environment. While high levels of mitotic missegregation would presumably have significant long-term consequences on a population's competitive fitness, a tolerance of high levels of meiotic missegregation may allow cells facing an uncertain future greater adaptive flexibility while imposing a lower fitness cost, as meiosis is a much rarer event than mitotic cell division in a yeast population. One function of meiosis is to generate new allelic combinations and greater phenotypic diversity in a population. Therefore, meiosis with a high frequency of chromosome missegregation may provide an independent source of further phenotypic variation in progeny (Ni *et al.* 2013), allowing adaptation to conditions that can be met only by allelic combinations that are vanishingly rare, if they exist at all. The existence of allele–aneuploidy interactions, as observed in our results, would have the effect of magnifying this phenotypic variation yet further.

Acknowledgments

We thank Eviatar Nevo, Justin Fay, Barak Cohen, Charles Boone, Fred Winston, and Timothy Galitski for providing strains and plasmids; Mark Johnston, Daniel Segrè, and Barak Cohen for helpful comments on the manuscript; and Scott Bloom and the Northwest Genomics Center for assistance with Illumina sequencing. This work was funded by National Institutes of Health/National Institute of General Medical Sciences grant R01 GM089978 (to A.M.D.) and by a strategic partnership between the Institute for Systems Biology and the University of Luxembourg.

Literature Cited

Acar, M., A. Becskei, and A. van Oudenaarden, 2005 Enhancement of cellular memory by reducing stochastic transitions. Nature 435: 228–232.

Akhabir, L., and A. J. Sandford, 2011 Genome-wide association studies for discovery of genes involved in asthma. Respirology 16: 396–406.

Antonarakis, S. E., and J. S. Beckmann, 2006 Mendelian disorders deserve more attention. Nat. Rev. Genet. 7: 277–282.

Baird, N. A., P. D. Etter, T. S. Atwood, M. C. Currey, A. L. Shiver *et al.*, 2008 Rapid SNP discovery and genetic mapping using sequenced RAD markers. PLoS ONE 3: e3376.

Bhat, P. J., 2008 Epistasis, pp. 87–89 in *Galactose Regulon of Yeast: From Genetics to Systems Biology*. Springer, Berlin.

Boles, E., and C. P. Hollenberg, 1997 The molecular genetics of hexose transport in yeasts. FEMS Microbiol. Rev. 21: 85–111.

Botstein, D., and G. R. Fink, 2011 Yeast: an experimental organism for 21st century biology. Genetics 189: 695–704.

Brinkman, R. R., M. P. Dube, G. A. Rouleau, A. C. Orr, and M. E. Samuels, 2006 Human monogenic disorders: a source of novel drug targets. Nat. Rev. Genet. 7: 249–260.

Broman, K. W., H. Wu, S. Sen, and G. A. Churchill, 2003 R/qtl: QTL mapping in experimental crosses. Bioinformatics 19: 889–890.

Chen, G., B. Rubinstein, and R. Li, 2012 Whole chromosome aneuploidy: big mutations drive adaptation by phenotypic leap. BioEssays 34: 893–900.

Coluccio, A., E. Bogengruber, M. N. Conrad, M. E. Dresser, P. Briza *et al.*, 2004 Morphogenetic pathway of spore wall assembly in Saccharomyces cerevisiae. Eukaryot. Cell 3: 1464–1475.

Cromie, G. A., K. E. Hyma, C. L. Ludlow, C. Garmendia-Torres, T. L. Gilbert *et al.*, 2013 Genomic sequence diversity and population

structure of *Saccharomyces cerevisiae* assessed by RAD-seq. G3 (Bethesda) 3: 2163–2171.
Cutting, G. R., 2010 Modifier genes in Mendelian disorders: the example of cystic fibrosis. Ann. N. Y. Acad. Sci. 1214: 57–69.
de Jongh, W. A., C. Bro, S. Ostergaard, B. Regenberg, L. Olsson *et al.*, 2008 The roles of galactitol, galactose-1-phosphate, and phosphoglucomutase in galactose-induced toxicity in Saccharomyces cerevisiae. Biotechnol. Bioeng. 101: 317–326.
Dipple, K. M., and E. R. McCabe, 2000a Modifier genes convert "simple" Mendelian disorders to complex traits. Mol. Genet. Metab. 71: 43–50.
Dipple, K. M., and E. R. McCabe, 2000b Phenotypes of patients with "simple" Mendelian disorders are complex traits: thresholds, modifiers, and systems dynamics. Am. J. Hum. Genet. 66: 1729–1735.
Donnini, C., T. Lodi, I. Ferrero, A. Algeri, and P. P. Puglisi, 1992 Allelism of IMP1 and GAL2 genes of Saccharomyces cerevisiae. J. Bacteriol. 174: 3411–3415.
Douglas, H. C., and D. C. Hawthorne, 1964 Enzymatic expression and genetic linkage of genes controlling galactose utilization in Saccharomyces. Genetics 49: 837–844.
Dunham, M. J., 2012 Two flavors of bulk segregant analysis in yeast. Methods Mol. Biol. 871: 41–54.
Egriboz, O., F. Jiang, and J. E. Hopper, 2011 Rapid GAL gene switch of *Saccharomyces cerevisiae* depends on nuclear Gal3, not nucleocytoplasmic trafficking of Gal3 and Gal80. Genetics 189: 825–836.
Ehrenreich, I. M., N. Torabi, Y. Jia, J. Kent, S. Martis *et al.*, 2010 Dissection of genetically complex traits with extremely large pools of yeast segregants. Nature 464: 1039–1042.
Ezov, T. K., E. Boger-Nadjar, Z. Frenkel, I. Katsperovski, S. Kemeny *et al.*, 2006 Molecular-genetic biodiversity in a natural population of the yeast *Saccharomyces cerevisiae* from "Evolution Canyon": microsatellite polymorphism, ploidy and controversial sexual status. Genetics 174: 1455–1468.
Fridovich-Keil, J. L., and S. Jinks-Robertson, 1993 A yeast expression system for human galactose-1-phosphate uridylyltransferase. Proc. Natl. Acad. Sci. USA 90: 398–402.
Genin, E., J. Feingold, and F. Clerget-Darpoux, 2008 Identifying modifier genes of monogenic disease: strategies and difficulties. Hum. Genet. 124: 357–368.
Gerke, J. P., C. T. Chen, and B. A. Cohen, 2006 Natural isolates of *Saccharomyces cerevisiae* display complex genetic variation in sporulation efficiency. Genetics 174: 985–997.
Goldstein, A. L., and J. H. McCusker, 1999 Three new dominant drug resistance cassettes for gene disruption in Saccharomyces cerevisiae. Yeast 15: 1541–1553.
Gupta, A., 2007 To err is genetics: diagnosis and management of inborn errors of metabolism (IEM), pp. 415–423 in *Anthropology Today: Trends, Scopes and Applications*, edited by V. Bhasin and M. K. Bhasin. Kamla-Raj Enterprises, New Delhi.
Guthrie, C., and G. R. Fink, 1991 *Guide to Yeast Genetics and Molecular Biology*. Academic Press, San Diego.
Herskowitz, I., and R. E. Jensen, 1991 Putting the HO gene to work: practical uses for mating-type switching. Methods Enzymol. 194: 132–146.
Hindorff, L. A., E. M. Gillanders, and T. A. Manolio, 2011 Genetic architecture of cancer and other complex diseases: lessons learned and future directions. Carcinogenesis 32: 945–954.
Johnston, M., 1987 A model fungal gene regulatory mechanism: the GAL genes of Saccharomyces cerevisiae. Microbiol. Rev. 51: 458–476.
Kar, R. K., M. T. Qureshi, A. K. DasAdhikari, T. Zahir, K. V. Venkatesh *et al.*, 2014 Stochastic galactokinase expression underlies GAL gene induction in a GAL3 mutant of Saccharomyces cerevisiae. FEBS J. 281: 1798–1817.
Katz Ezov, T., S. L. Chang, Z. Frenkel, A. V. Segre, M. Bahalul *et al.*, 2010 Heterothallism in Saccharomyces cerevisiae isolates from nature: effect of HO locus on the mode of reproduction. Mol. Ecol. 19: 121–131.
Knowles, M. R., 2006 Gene modifiers of lung disease. Curr. Opin. Pulm. Med. 12: 416–421.
Ko, C. H., H. Liang, and R. F. Gaber, 1993 Roles of multiple glucose transporters in Saccharomyces cerevisiae. Mol. Cell. Biol. 13: 638–648.
Koller, A., J. Heitman, and M. N. Hall, 1996 Regional bivalent-univalent pairing *vs.* trivalent pairing of a trisomic chromosome in *Saccharomyces cerevisiae*. Genetics 144: 957–966.
Lander, E. S., and D. Botstein, 1989 Mapping mendelian factors underlying quantitative traits using RFLP linkage maps. Genetics 121: 185–199.
Lango Allen, H., K. Estrada, G. Lettre, S. I. Berndt, M. N. Weedon *et al.*, 2010 Hundreds of variants clustered in genomic loci and biological pathways affect human height. Nature 467: 832–838.
Larschan, E., and F. Winston, 2005 The Saccharomyces cerevisiae Srb8-Srb11 complex functions with the SAGA complex during Gal4-activated transcription. Mol. Cell. Biol. 25: 114–123.
Leslie, N. D., 2003 Insights into the pathogenesis of galactosemia. Annu. Rev. Nutr. 23: 59–80.
Li, H., and R. Durbin, 2009 Fast and accurate short read alignment with Burrows-Wheeler transform. Bioinformatics 25: 1754–1760.
Li, H., B. Handsaker, A. Wysoker, T. Fennell, J. Ruan *et al.*, 2009 The Sequence Alignment/Map format and SAMtools. Bioinformatics 25: 2078–2079.
Liang, H., and R. F. Gaber, 1996 A novel signal transduction pathway in Saccharomyces cerevisiae defined by Snf3-regulated expression of HXT6. Mol. Biol. Cell 7: 1953–1966.
Lohr, D., P. Venkov, and J. Zlatanova, 1995 Transcriptional regulation in the yeast GAL gene family: a complex genetic network. FASEB J. 9: 777–787.
Lorenz, K., and B. A. Cohen, 2012 Small- and large-effect quantitative trait locus interactions underlie variation in yeast sporulation efficiency. Genetics 192: 1123–1132.
Ludlow, C. L., A. C. Scott, G. A. Cromie, E. W. Jeffery, A. Sirr *et al.*, 2013 High-throughput tetrad analysis. Nat. Methods 10: 671–675.
Mancera, E., R. Bourgon, A. Brozzi, W. Huber, and L. M. Steinmetz, 2008 High-resolution mapping of meiotic crossovers and non-crossovers in yeast. Nature 454: 479–485.
Marian, A. J., and J. Belmont, 2011 Strategic approaches to unraveling genetic causes of cardiovascular diseases. Circ. Res. 108: 1252–1269.
Mayatepek, E., B. Hoffmann, and T. Meissner, 2010 Inborn errors of carbohydrate metabolism. Best Pract. Res. Clin. Gastroenterol. 24: 607–618.
McCorvie, T. J., and D. J. Timson, 2011 The structural and molecular biology of type I galactosemia: enzymology of galactose 1-phosphate uridylyltransferase. IUBMB Life 63: 694–700.
Mehta, D. V., A. Kabir, and P. J. Bhat, 1999 Expression of human inositol monophosphatase suppresses galactose toxicity in Saccharomyces cerevisiae: possible implications in galactosemia. Biochim. Biophys. Acta 1454: 217–226.
Michelmore, R. W., I. Paran, and R. V. Kesseli, 1991 Identification of markers linked to disease-resistance genes by bulked segregant analysis: a rapid method to detect markers in specific genomic regions by using segregating populations. Proc. Natl. Acad. Sci. USA 88: 9828–9832.
Mumma, J. O., J. S. Chhay, K. L. Ross, J. S. Eaton, K. A. Newell-Litwa *et al.*, 2008 Distinct roles of galactose-1P in galactose-mediated growth arrest of yeast deficient in galactose-1P uridylyltransferase (GALT) and UDP-galactose 4′-epimerase (GALE). Mol. Genet. Metab. 93: 160–171.
Nadeau, J. H., 2001 Modifier genes in mice and humans. Nat. Rev. Genet. 2: 165–174.
Nadeau, J. H., 2003 Modifier genes and protective alleles in humans and mice. Curr. Opin. Genet. Dev. 13: 290–295.

Ni, M., M. Feretzaki, W. Li, A. Floyd-Averette, P. Mieczkowski *et al.*, 2013 Unisexual and heterosexual meiotic reproduction generate aneuploidy and phenotypic diversity de novo in the yeast Cryptococcus neoformans. PLoS Biol. 11: e1001653.

Nogi, Y., K. Matsumoto, A. Toh-e, and Y. Oshima, 1977 Interaction of super-repressible and dominant constitutive mutations for the synthesis of galactose pathway enzymes in Saccharomyces cerevisiae. Mol. Gen. Genet. 152: 137–144.

Nogi, Y., H. Shimada, Y. Matsuzaki, H. Hashimoto, and T. Fukasawa, 1984 Regulation of expression of the galactose gene cluster in Saccharomyces cerevisiae. II. The isolation and dosage effect of the regulatory gene GAL80. Mol. Gen. Genet. 195: 29–34.

Parts, L., F. A. Cubillos, J. Warringer, K. Jain, F. Salinas *et al.*, 2011 Revealing the genetic structure of a trait by sequencing a population under selection. Genome Res. 21: 1131–1138.

Pavelka, N., G. Rancati, J. Zhu, W. D. Bradford, A. Saraf *et al.*, 2010 Aneuploidy confers quantitative proteome changes and phenotypic variation in budding yeast. Nature 468: 321–325.

Polakova, S., C. Blume, J. A. Zarate, M. Mentel, D. Jorck-Ramberg *et al.*, 2009 Formation of new chromosomes as a virulence mechanism in yeast Candida glabrata. Proc. Natl. Acad. Sci. USA 106: 2688–2693.

Polychronakos, C., and Q. Li, 2011 Understanding type 1 diabetes through genetics: advances and prospects. Nat. Rev. Genet. 12: 781–792.

R Core Team, 2013 R: A language and environment for statistical computing. *R Foundation for Statistical Computing*, Vienna, Austria. Available at: http://www.R-project.org/.

Rancati, G., N. Pavelka, B. Fleharty, A. Noll, R. Trimble *et al.*, 2008 Aneuploidy underlies rapid adaptive evolution of yeast cells deprived of a conserved cytokinesis motor. Cell 135: 879–893.

Reedy, J. L., A. M. Floyd, and J. Heitman, 2009 Mechanistic plasticity of sexual reproduction and meiosis in the Candida pathogenic species complex. Curr. Biol. 19: 891–899.

Reifenberger, E., E. Boles, and M. Ciriacy, 1997 Kinetic characterization of individual hexose transporters of Saccharomyces cerevisiae and their relation to the triggering mechanisms of glucose repression. Eur. J. Biochem. 245: 324–333.

Rose, M. D., F. M. Winston, and P. Hieter, 1990 *Methods in Yeast Genetics: A Laboratory Course Manual*. Cold Spring Harbor Laboratory Press, Cold Spring Harbor, NY.

Scott, A. C., C. L. Ludlow, G. A. Cromie, and A. M. Dudley, 2014 BEST: barcode enabled sequencing of tetrads. J. Vis. Exp. (87), e51401, doi:10.3791/51401.

Segre, A. V., A. W. Murray, and J. Y. Leu, 2006 High-resolution mutation mapping reveals parallel experimental evolution in yeast. PLoS Biol. 4: e256.

Selmecki, A., A. Forche, and J. Berman, 2006 Aneuploidy and isochromosome formation in drug-resistant Candida albicans. Science 313: 367–370.

Selmecki, A. M., K. Dulmage, L. E. Cowen, J. B. Anderson, and J. Berman, 2009 Acquisition of aneuploidy provides increased fitness during the evolution of antifungal drug resistance. PLoS Genet. 5: e1000705.

Sionov, E., H. Lee, Y. C. Chang, and K. J. Kwon-Chung, 2010 Cryptococcus neoformans overcomes stress of azole drugs by formation of disomy in specific multiple chromosomes. PLoS Pathog. 6: e1000848.

Sniegowski, P. D., P. G. Dombrowski, and E. Fingerman, 2002 Saccharomyces cerevisiae and Saccharomyces paradoxus coexist in a natural woodland site in North America and display different levels of reproductive isolation from European conspecifics. FEMS Yeast Res. 1: 299–306.

Sora, S., G. Lucchini, and G. E. Magni, 1982 Meiotic diploid progeny and meiotic nondisjunction in *Saccharomyces cerevisiae*. Genetics 101: 17–33.

St. Charles, J., M. L. Hamilton, and T. D. Petes, 2010 Meiotic chromosome segregation in triploid strains of *Saccharomyces cerevisiae*. Genetics 186: 537–550.

Tan, Z., M. Hays, G. A. Cromie, E. W. Jeffery, A. C. Scott *et al.*, 2013 Aneuploidy underlies a multicellular phenotypic switch. Proc. Natl. Acad. Sci. USA 110: 12367–12372.

Tang, M., S. I. Odejinmi, H. Vankayalapati, K. J. Wierenga, and K. Lai, 2012 Innovative therapy for classic galactosemia: tale of two HTS. Mol. Genet. Metab. 105: 44–55.

Thorburn, R. R., C. Gonzalez, G. A. Brar, S. Christen, T. M. Carlile *et al.*, 2013 Aneuploid yeast strains exhibit defects in cell growth and passage through START. Mol. Biol. Cell 24: 1274–1289.

Tong, A., and C. Boone, 2005 *Yeast Protocols*. The Humana Press, Totowa, NJ.

Tong, A. H., M. Evangelista, A. B. Parsons, H. Xu, G. D. Bader *et al.*, 2001 Systematic genetic analysis with ordered arrays of yeast deletion mutants. Science 294: 2364–2368.

Torchia, T. E., and J. E. Hopper, 1986 Genetic and molecular analysis of the GAL3 gene in the expression of the galactose/melibiose regulon of *Saccharomyces cerevisiae*. Genetics 113: 229–246.

Torres, E. M., T. Sokolsky, C. M. Tucker, L. Y. Chan, M. Boselli *et al.*, 2007 Effects of aneuploidy on cellular physiology and cell division in haploid yeast. Science 317: 916–924.

Wach, A., A. Brachat, R. Pohlmann, and P. Philippsen, 1994 New heterologous modules for classical or PCR-based gene disruptions in Saccharomyces cerevisiae. Yeast 10: 1793–1808.

Weatherall, D. J., 2001 Phenotype-genotype relationships in monogenic disease: lessons from the thalassaemias. Nat. Rev. Genet. 2: 245–255.

Weiler, C. A., and M. L. Drumm, 2013 Genetic influences on cystic fibrosis lung disease severity. Front Pharmacol 4: 40.

Wieczorke, R., S. Krampe, T. Weierstall, K. Freidel, C. P. Hollenberg *et al.*, 1999 Concurrent knock-out of at least 20 transporter genes is required to block uptake of hexoses in Saccharomyces cerevisiae. FEBS Lett. 464: 123–128.

Wilkening, S., G. Lin, E. S. Fritsch, M. M. Tekkedil, S. Anders *et al.*, 2013 An evaluation of high-throughput approaches to QTL mapping in *Saccharomyces cerevisiae*. Genetics 196: 853–865.

Xiao, W., 2006 *Yeast Protocols*. Humana Press, Totowa, NJ.

Yona, A. H., Y. S. Manor, R. H. Herbst, G. H. Romano, A. Mitchell *et al.*, 2012 Chromosomal duplication is a transient evolutionary solution to stress. Proc. Natl. Acad. Sci. USA 109: 21010–21015.

Communicating editor: L. M. Steinmetz

GENETICS

Supporting Information
http://www.genetics.org/lookup/suppl/doi:10.1534/genetics.114.170563/-/DC1

Allelic Variation, Aneuploidy, and Nongenetic Mechanisms Suppress a Monogenic Trait in Yeast

Amy Sirr, Gareth A. Cromie, Eric W. Jeffery, Teresa L. Gilbert, Catherine L. Ludlow, Adrian C. Scott, and Aimée M. Dudley

DOI: 10.1534/genetics.114.170563

Table S1 Strain doubling times in galactose and raffinose shown with standard errors

Strain	YP + 2% galactose + 1mg/mL antimycin A	YP + 2% galactose + 2%raffinose + 1mg/mL antimycin A
EC33	**221 +/- 5 min**	**222 +/- 5 min**
EC33-gal	**No growth**	**No growth**
YPS163	**217 +/- 4 min**	**209 +/- 4 min**
YPS163-gal	**No growth**	**No growth**
EC33-gal x YPS163-gal	**No growth**	**No growth**
FY4	**240 +/- 2 min**	**237 +/- 2 min**

Table S2 Survival frequencies of mitotically and meiotically derived galactose tolerant clones

Progenitor	Strain	URA	Plating method	Viability on galactose	Percent viable on galactose
YPG3161	YO1652	-	FACS QTL sorted spores	**42/627**	**7%**
YPG3161	YO1652	-	Hand dissected spores	**4/40**	**10%**
YPG3161	YPG3161 clone	+	FACS sorted single cells	**27/92**	**29%**
YPG3161	YO2124	-	FACS sorted single cells	**24/92**	**26%**
YPG3140	YO1650	-	FACS QTL sorted spores	**63/633**	**10%**
YPG3140	YO1650	-	Hand dissected spores	**7/40**	**18%**
YPG3140	YPG3140 clone	+	FACS sorted single cells	**36/92**	**39%**
YPG3140	YO2123	-	FACS sorted single cells	**17/92**	**18%**

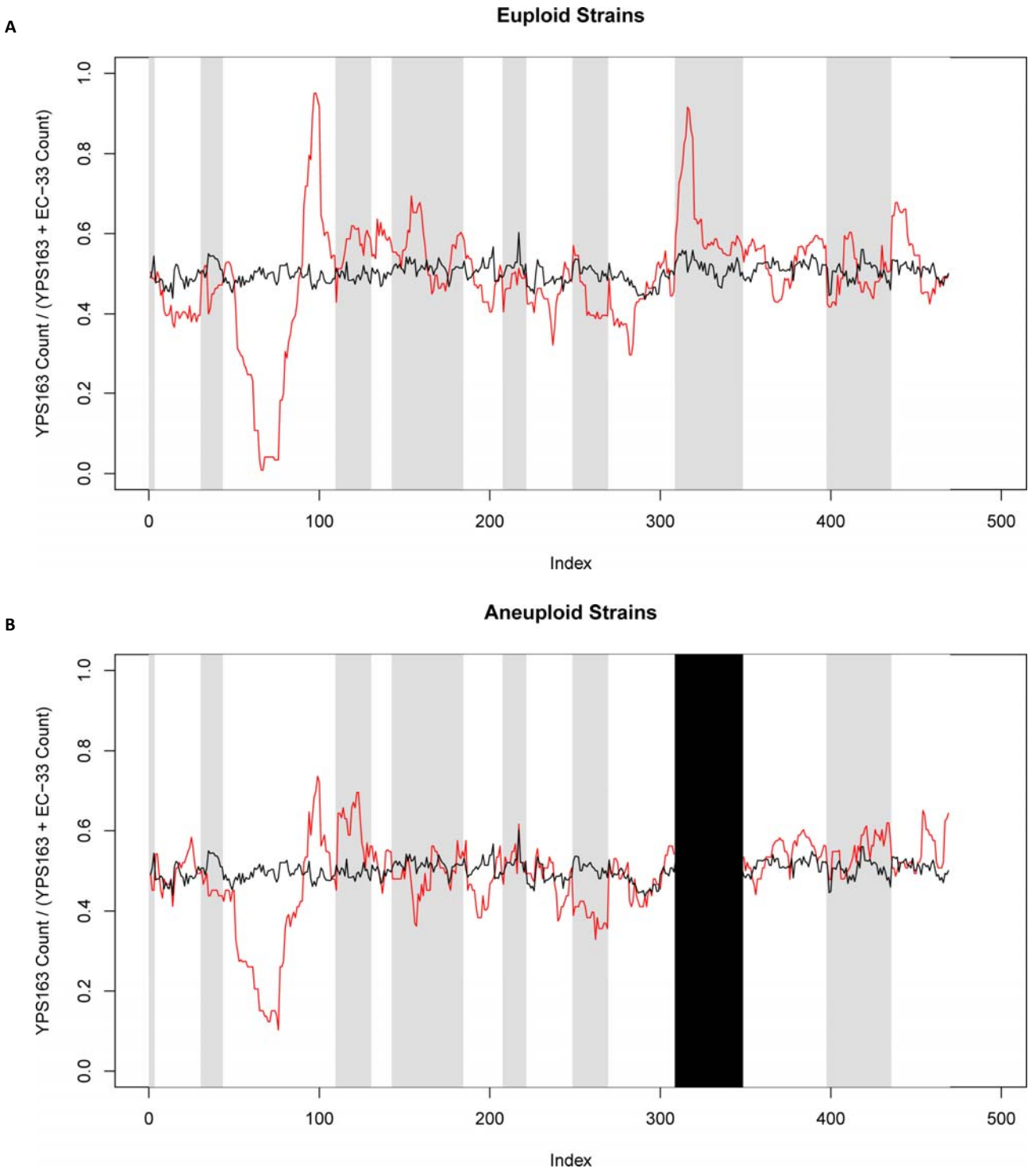

Figure S1 Allele frequencies in the selected (red) and unselected (black) populations in the **A)** euploid and **B)** aneuploid classes of galactose tolerant segregants from the EC33-gal x YPS163-gal cross.

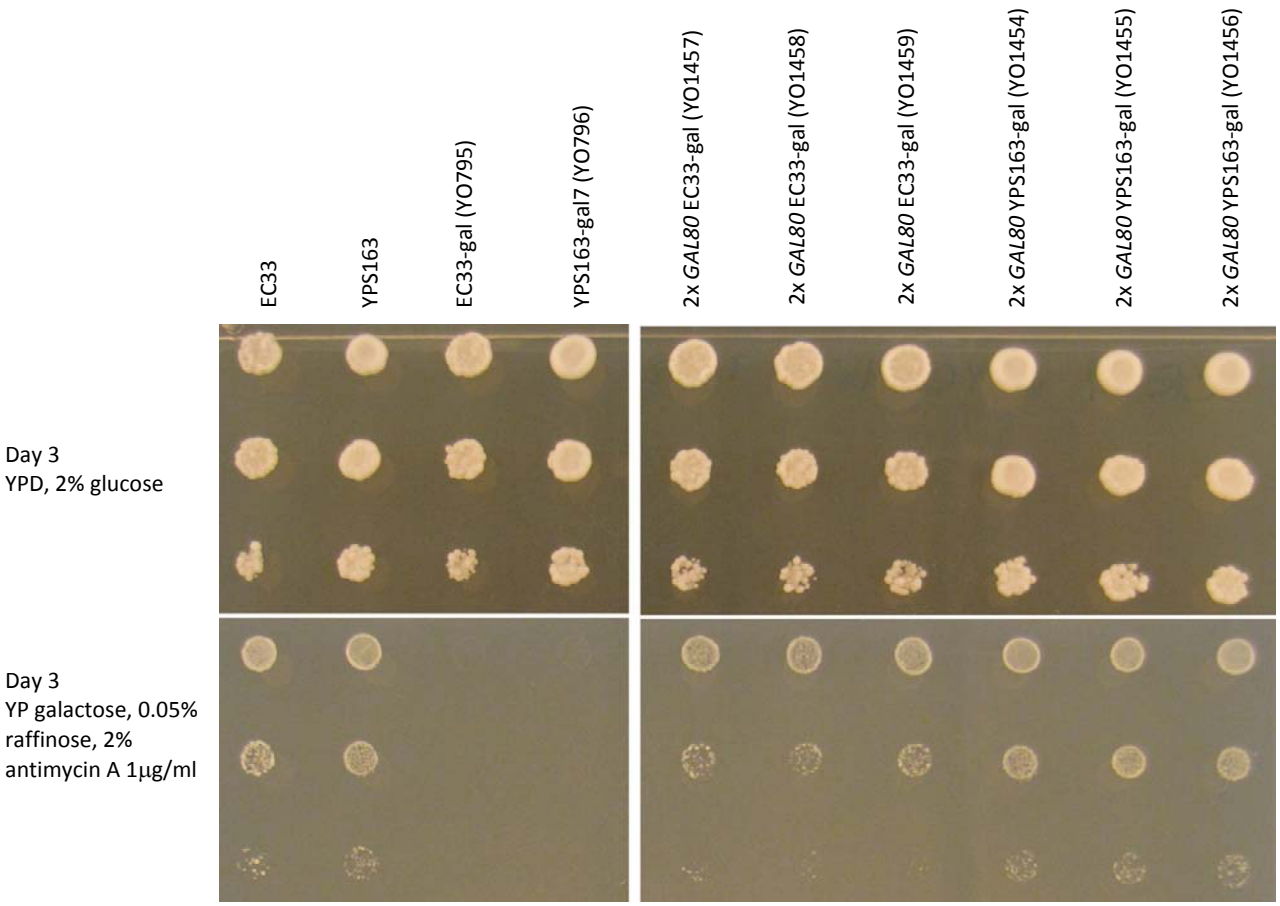

Figure S2 Gene dosage effect of *GAL80*

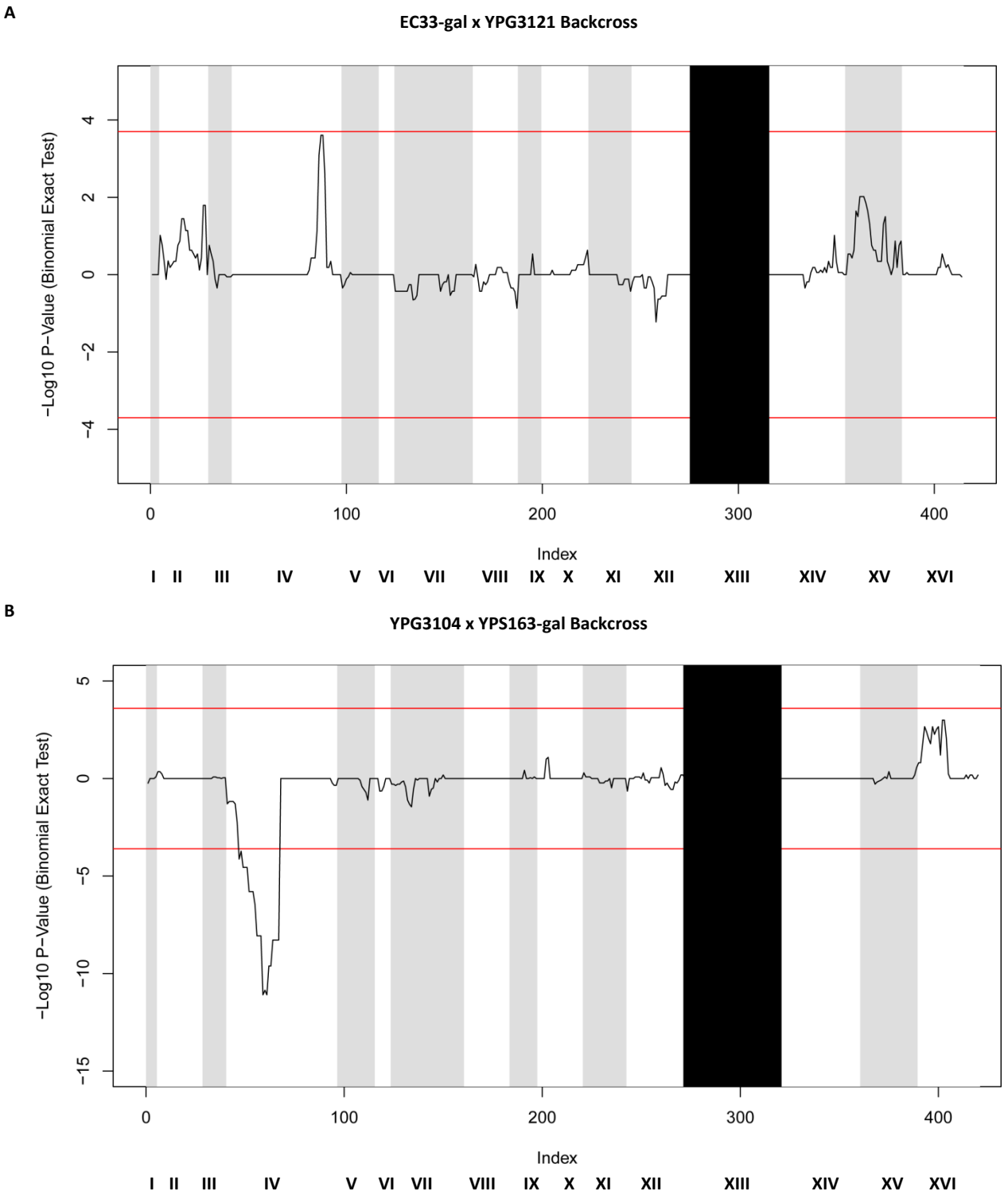

Figure S3 QTL mapping of galactose tolerant progeny from chromosome XIII F1 progeny backcrosses

File S1

Genomic changes between reference strain and whole genome sequencing of EC-33 and YPS163

File S1 is available for download as a .xlsx file at
http://www.genetics.org/lookup/suppl/doi:10.1534/genetics.114.170563/-/DC1

File S2

Allele table of EC33-gal x YPS163-gal progeny grown on galactose

File S2 is available for download as a .xlsx file at
http://www.genetics.org/lookup/suppl/doi:10.1534/genetics.114.170563/-/DC1

File S3

Ploidy estimates of EC33-gal x YPS163-gal progeny grown on galactose

File S3 is available for download as a .xlsx file at
http://www.genetics.org/lookup/suppl/doi:10.1534/genetics.114.170563/-/DC1

File S4

QTL mapping p-values at each marker position for galactose tolerant euploid and chromosome XIII disomic progeny of EC33-gal x YPS163-gal cross

File S4 is available for download as a .xlsx file at
http://www.genetics.org/lookup/suppl/doi:10.1534/genetics.114.170563/-/DC1

File S5

3-way comparison between reference strain, EC-33 and YPS163 in *HXT6, 7* regions

File S5 is available for download as a .doc file at
http://www.genetics.org/lookup/suppl/doi:10.1534/genetics.114.170563/-/DC1

File S6

Ploidy estimates of EC33-gal x YPS163-gal control progeny grown on YPD

File S6 is available for download as a .xlsx file at
http://www.genetics.org/lookup/suppl/doi:10.1534/genetics.114.170563/-/DC1

File S7

Ploidy analysis for progeny of backcrosses between parent strains and F1 progeny with chromosome XIII disomy

File S7 is available for download as a .xlsx file at
http://www.genetics.org/lookup/suppl/doi:10.1534/genetics.114.170563/-/DC1

File S8

Sequence Read Archive repository accession numbers

PRJEB7308: RAD-seq genotyping of galactose-tolerant progeny from a backcross between disomic strain YPG3121 (chromosome XIII disome) and parent YO795 is available for download at http://www.ncbi.nlm.nih.gov/bioproject/PRJEB7308

PRJEB7309: RAD-seq genotyping of galactose-tolerant progeny from a backcross between disomic strain YPG3104 (chromosome XIII disome) and parent YO796 is available for download at http://www.ncbi.nlm.nih.gov/bioproject/PRJEB7309

PRJEB7334: RAD-seq genotyping of progeny from a cross between strains YO795 (EC-33) and YO796 (YPS163) is available for download at

http://www.ncbi.nlm.nih.gov/bioproject/PRJEB7334

PRJEB7336: RAD-seq genotyping of galactose-tolerant progeny from a cross between strains YO795 (EC-33) and YO796 (YPS163) is available for download at http://www.ncbi.nlm.nih.gov/bioproject/PRJEB7336

PRJEB7586: Whole genome sequencing of Pennsylvania yeast strain YO516 (YPS163, NV43) isolated from Oak tree is available for download at

http:/www.ncbi.nlm.nih.gov/bioproject/PRJEB7586

PRJEB7587: Whole genome sequencing of yeast strain YO528 (EC-33, NV 57) isolated from Evolution Canyon, Israel is available for download at

http://www.ncbi.nlm.nih.gov/bioproject/PRJEB7587